SYNTHESIS OF ALINITE CEMENT USING SODA SOLID WASTE

A THESIS SUBMITTED TO
THE GRADUATE SCHOOL OF NATURAL AND APPLIED SCIENCES
OF
MIDDLE EAST TECHNICAL UNIVERSITY

BY

ASLI GÜNEŞ

IN PARTIAL FULFILLMENT OF THE REQUIREMENTS
FOR
THE DEGREE OF MASTER OF SCIENCE
IN
CEMENT ENGINEERING

SEPTEMBER 2010

Approval of the thesis:

SYNTHESIS OF ALINITE CEMENT USING SODA SOLID WASTE

submitted by **ASLI GÜNEŞ** in partial fulfillment of the requirements for the **Degree of Master of Science in Cement Engineering**, **Middle East Technical University** by,

Prof. Dr. Canan Özgen _____
Dean, Graduate School of **Natural and Applied Sciences**

Prof. Dr. Asuman Türkmenoğlu _____
Head of Department, **Cement Eng. Dept., METU**

Assoc. Prof. Dr. İ. Özgür Yaman _____
Supervisor, **Civil Eng. Dept., METU**

Prof. Dr. Abdullah Öztürk _____
Co-Supervisor, **Metallurgical and Materials Eng. Dept., METU**

Examining Committee Members:

Prof. Dr. Mustafa Tokyay _____
Civil Eng. Dept., METU

Prof. Dr. Çetin Hoşten _____
Mining Eng. Dept., METU

Prof. Dr. Abdullah Öztürk _____
Metallurgical and Materials Eng. Dept., METU

Assoc. Prof. Dr. İ. Özgür Yaman _____
Civil Eng. Dept., METU

Assoc. Prof. Dr. Ömer Kuleli _____
Cement Eng. Dept., METU

Date: 15.09.2010

I hereby declare that all information in this document has been obtained and presented in accordance with academic rules and ethical conduct. I also declare that, as required by these rules and conduct, I have fully cited and referenced all material and results that are not original to this work.

Name, Last Name:

Signature :

ABSTRACT

SYNTHESIS OF ALINITE CEMENT USING SODA SOLID WASTE

Güneş, Aslı
MSc., Department of Cement Engineering
Supervisor: Assoc. Prof. Dr. İ.Özgür Yaman
Co-Supervisor: Prof. Dr. Abdullah Öztürk

September 2010, 52 pages

This study is dedicated to give a production route for a kind of low energy cement called alinite cement using the waste material of soda industry as the main raw material.

Soda solid waste, clay and minor amount of iron ore were mixed with certain quantities and burned at six different burning temperatures of 1050, 1100, 1150, 1200, 1350, and 1450 ºC. The resultant clinkers were investigated by mineralogical and chemical analysis. Mineralogical analyses were performed by X-Ray Diffraction (XRD) technique. XRD analyses revealed the formation of alinite phase in the clinkers. Chemical analyses were performed by X-Ray Fluorescence spectroscopy technique and by wet chemical analysis. Especially, free lime content of the clinkers was searched and an optimum burning temperature was determined.

In order to find the compressive strength of the alinite cement, larger amounts of alinite clinker were manufactured in wet rod shape raw mix in a laboratory type of furnace at 1200, 1350 and 1450 ºC.

The results have shown that forming alinite phase requires ~6wt % chlorine. Alinite clinker is obtained using soda waste at the temperature range between 1050 and 1200 ºC. However, the free CaO becomes much lower as 0.12 at 1200 ºC. Moreover, a lime saturation factor of 76, which is lower than ordinary Portland clinker is obtained. Satisfactory compressive strength was achieved by gypsum addition.

Keywords: Alinite, alinite cement, low energy cement, soda solid waste

ÖZ

SODA SANAYİSİ KATI ATIĞI İLE ALİNİT ÇİMENTOSU SENTEZİ

Güneş, Aslı
Yüksek Lisans, Çimento Mühendisliği
Tez Yöneticisi: Doç. Dr. İ.Özgür Yaman
Ortak Tez Yöneticisi: Prof. Dr. Abdullah Öztürk

Eylül 2010, 52 sayfa

Bu çalışma, bir çeşit düşük enerjili çimento olan alinit çimentosunun temel ham madde olarak soda sanayisi atığı kullanılarak üretim yöntemini sunmaktadır.

Soda katı atığı, kil ve düşük miktarda demir cevheri ile belirli bir oranda farin hazırlanmış ve altı değişik yanma sıcaklığında 1050, 1100, 1150, 1200, 1350 ve 1450 ºC pişirilmiştir. Oluşan klinker numuneleri mineralojik ve kimyasal analizlere tabii tutulmuştur. Mineralojik analiz X-Işınları Difraktometri tekniği ile incelenmiştir. Yapılan analizlerde, klinker içinde alinit fazının oluştuğu görülmüştür. Kimyasal analizler X-Işınları Floresans spektroskopisi yöntemi ve kimyasal yaş metotlarla yapılmıştır. Özellikle, serbest kireç tayini sonuçları da incelenerek optimum yanma sıcaklığı belirlenmiştir.

Alinit çimentosuna ait basınç dayanımı tayini için fazla miktarda klinker, ıslatılarak çubuk şekline getirilen farinin laboratuar tipi bir fırın kullanılarak 1200, 1350 ve 1450ºC sıcaklıklarda pişme sıcaklığında üretilmiştir.

Elde edilen sonuçlar alinit fazının oluşabilmesi için yüksek klor (~6%kütlece) gerektiğini göstermiştir. Alinit klinkeri, soda atığının 1050 ve 1200 ºC sıcaklıkları arasında elde edilmiştir. Fakat, 1200 ºC sıcaklıkta pişme ile serbest kireç değerleri 0.12 gibi oldukça düşük çıkmıştır. Ayrıca, normal Portland Çimentosu'na oranla daha düşük olarak 76 kireç modülü ile üretilmiştir. Yeterli dayanım değerleri alçı taşı katkısı ile elde edildiği görülmüştür.

Anahtar Kelimeler: Alinit, alinit çimentosu, düşük enerjili çimento, soda katı atık

ACKNOWLEDGMENTS

I would like to express my gratitude to Assoc. Prof. Dr. İ. Özgür Yaman for his supervision and suggestion throughout this research and preparation of this thesis.

I am also thankful to my co-supervisor Prof. Abdullah Öztürk and Assoc. Prof. Dr. Ömer Kuleli for their encouragement to study in cement engineering department.

Deep appreciation and thanks are due to Prof. Dr. Mustafa Tokyay, who has given me the belief of success and without his personal interest and support the thesis would have not been completed. His guidance will never be forgotten.

I would like to thank Didem Benzer, Serkan Türk, Tuğhan Delibaş, Pelin Ayturan and other colleagues in Turkish Cement Manufacturers' Association for their contributions.

I am also thankful to Mersin Soda Plant for providing their waste material.

Finally, I am also grateful to my family and my fiancé for their invaluable support.

TABLE OF CONTENTS

LIST OF TABLES

TABLES

LIST OF FIGURES

FIGURES

LIST OF ABBREVIATIONS

AAS	: Atomic Absorption Spectroscopy
AM	: Alumina Module
EDS	: Energy Dispersive X-Ray Spectroscopy
h	: Hour
LSF	: Lime Saturation Factor
LOI	: Loss on Ignition
min	: Minute
MPa	: Mega Pascal
SEM	: Scanning Electron Microscope
SM	: Silica Module
w/c	: Water/Cement ratio
wt%	: Weight percentage
XRD	: X-Ray Diffraction
XRF	: X-Ray Fluorescence

CHAPTER 1

INTRODUCTION

1.1 General

Alinite cement is a special type of low energy cement which is mainly composed of a silicate phase with mixed oxygen-chlorine anions. The lattice structure of the alinite phase has the ability to accommodate Cl^- ions, thus minimize the deleterious effects to steel reinforcing bars. Based on the chemistry of alinite compound, it is suitable to convert a wide variety of industrial wastes or by-products such as fly ashes and other minerals into a new class of hydraulic setting alinite cements [Pradip and Kapur, 1990].

Alinite cement can be produced by various industrial waste products such as steel plant waste, chlorine containing by by-products etc [Odler, 2000]. One of the suitable waste materials is soda solid waste coming out of the Solvay process. The main reason for selecting this waste is its relatively high chlorine content. Alinite cement with different raw mix modules, burning schemes and XRD patterns serves as a new low energy cement to the sector.

Besides the well known industries such as steel industry and thermal power plants, soda industry is a potential candidate to provide its waste as an alternative raw material to the cement industry.

The most common way of soda production is Solvay Process. The products are sodium carbonate, calcium chloride and solid waste which is mainly unburnt calcium carbonate, sand and clays from the kiln. The waste form huge sludge deposits, although it is not toxic, becomes a problem as it occupies large space and creates environmental pollution.

1.2 Research Objectives and Scope

The objective of this experimental study is to produce alinite cement by using the soda waste as the main raw material. Besides the soda solid waste, clay and minor amounts of iron ore were also used. A proper lime saturation factor, silica and alumina modules were selected and the raw meal was subjected to different burning temperatures. The optimum burning temperature was determined by examining the characteristic peaks of the alinite clinker phases that were detected by X-Ray Diffractometer (XRD).

Within the scope of the experimental program, the raw mixture was subjected to eleven different burning schemes. The clinkers were produced in platinum crucible. The burning temperatures are chosen as 1050, 1100, 1150, 1200, 1350 and 1450 ºC. Samples burned at 1350 and 1450 ºC have burning duration of 10 minutes whereas for other temperatures burning duration were both 60 and 90 minutes. In order to find the compressive strength of the hardened alinite mortar, additional burning trials were also performed in relatively larger quantities at burning temperatures of 1200, 1350 and 1450 ºC.

Chapter 2 includes the idea of low energy cements, the theory and basic steps of Solvay process, the history and chemistry of Alinite Cements, raw meal optimization and the theory X-Ray Diffraction (XRD).

In chapter 3, starting from the preparation of the raw meal to the burned clinker, all steps of the experiments of chemical analyses, XRD, physical and mechanical analyses and scanning electron microscopy (SEM) are introduced.

In chapter 4, the results are given in the subtitles of chemical properties, including the main oxide compounds, mineralogical properties, including the XRD results, physical and mechanical properties and SEM results.

In chapter 5, conclusions and recommendation for future studies are presented to guide the future studies about this subject.

CHAPTER 2

LITERATURE REVIEW AND BACKROUND

2.1 Low-Energy Cements

The tendency towards sustainable development forces people in cement industry to consider the undesired effects of the high temperature process and the raw meal consumption. The term “low-energy cements” designates the alternative cement type for ordinary Portland cement with a reduced consumption of energy. Low-energy cements are mainly produced from the incineration ash produced in the incineration of the municipal waste, from sewage sludge and from other waste materials, especially those that contain distinct amounts of chlorine [Locher, 1986]. The main reason for producing this kind of cement is to avoid the necessity of disposing these wastes and to utilize them as raw materials for a technically useful product. Therefore, these wastes are most often termed as industrial by-products.

2.2 Solvay Process of Soda Production

The Solvay process, also referred to as the ammonia-soda process, has been the major industrial process used in the production of soda ash (sodium carbonate) for nearly 125 years [Roebuck, 2004]. Soda ash itself is among the most important products produced by the chemical industry, and is used in enormous quantities to manufacture glass and other products. A very large scale of its manufacture in the order of 40 million tons per year worldwide, the local availability of raw materials,

the price of energy, and the environmental impact of its production, are key drivers for improvements in the soda industry worldwide. The ammonia-soda process also called Solvay process was developed into essentially its modern form by Ernest Solvay in the 1860's [Soda Process Bref, 2004].

The Solvay process produces soda ash (predominantly sodium carbonate, Na_2CO_3) from brine (as a source of sodium chloride, NaCl) and from limestone (as a source of calcium carbonate, $CaCO_3$). The overall process is given as reaction (1) [Roebuck, 2004]:

$$2\ NaCl + CaCO_3 \rightarrow Na_2CO_3 + CaCl_2 \qquad (1)$$

When properly designed and operated, a Solvay plant can reclaim almost all its ammonia, and consumes only small amounts of additional ammonia to make up for losses. The only major inputs to the Solvay process are salt and limestone, and its only major byproduct is calcium chloride [Roebuck, 2004]. The solution left behind is a waste known as hot effluent and contains some CaO, $CaCO_3$, and $CaSO_4$ in addition to NH_4Cl and NaCl [Sharma et al., 2004].

The soda industry in Turkey provides soda (soda ash) to glass, detergent, textile and paper industries. Part of byproducts is recovered into the process at different parts of the process. However, one of the principle by-product soda sludge or called soda solid waste– Calcium Chloride ($CaCl_2$) in aqueous solution- has limited use due to its drying cost, high chlorine content, etc. Distiller waste of the soda ash plant contains about 2% of solids. Some of the synthetic soda ash producers in Europe discharge their distiller waste directly to the sea or river. Settling pond are abandoned and replanted for daily usage when filled with solid particles [Gür et al., 2010]. For 1 tone soda ash production about 330 kg of solid waste comes out [Sharma et al., 2004]. The soda sludge consists of mainly $CaCO_3$, $CaSO_4$, $Mg(OH)_2$, SiO_2, Al_2O_3 and $Ca(OH)_2$. The main drawback of the material is its relatively high chlorine content (~%6). Chlorine level can be decreased down to %1 by a washing method. However, in the case of alinite cement high chlorine content is required. Due to its similar composition soda solid waste becomes an alternative raw material for alinite cement synthesis.

2.3 Alinite Cement

Alinite Cement is a special type of low-energy cement. It was developed in the former Soviet Union, and was patented by Noudelman in 1977 [Hewlett, 2004]. $CaCl_2$ added to the Portland cement clinker raw feed forms chloralinite ($Ca_{11}Si_3AlO_{18}Cl$) [Hewlett, 2004]. There are some industrial companies from India, Russia and Japan who produces alinite cement [Gür et al., 2010]. It is characterized by the presence of the alinite phase in clinker instead of alite.

Alinite clinker may be produced from a raw meal containing limestone, clay, MgO and $CaCl_2$ (6-18 weight percentage, wt %) by burning it to temperatures of 1000-1300°C. A variety of industrial waste products, such as fly ash, magnesite dust, steel plant wastes or municipal waste with a significant amount of chlorine-containing materials may also be utilized as raw meal constituents [Pradip and Kapur, 1990]. The overall saving in energy in the production of alinite cements is ~1250kJ/kg, amounting to a 30 % saving [Locher, 1986]. Some chloride evaporates in the kiln and may give rise to a chloride cycle in the kiln.

Alinite phase is stable at a temperature range of 900-1150 °C and the actual clinkerization is carried out at 1150-1200 °C range with heat consumption of about 535 kcal/kg clinker (2239 kJ/kg clinker) [Benstend and Barnes, 1994]. The chemical composition of alinite cement and ordinary Portland cement are shown in Table 1. Alinite cement contains lesser amount of CaO and larger amount of Al_2O_3 and Fe_2O_3 than Portland cement.

Table 1 Ranges of Chemical composition for Alinite and Portland cements [Hewlett, 2004]

Constituent (wt%)	Alinite Cement	Portland Cement
CaO	45-55	62-67
SiO_2	13-19	18-24
Al_2O_3	9-12	4-8
Fe_2O_3	4-10	1.5-4.5
MgO	1-10	0.5-4
$CaCl_2$	6-8	-
Limestone used to form clinker	60-70	75-80

The alinite clinkers are always soft and friable due to weak Ca-Cl bonds. Therefore, grinding energy will be less for these cements. Greater fineness can be obtained with lower energy consumption. The enhanced specific surface area imparts, as expected the superior workability to cement pastes as well as higher strengths [Pradip and Kapur, 2004].

2.3.1 Mineralogical Composition of Alinite Cement

The range of variations of the composition of the industrially produced alinite clinker is presented in Table 2.

The clinker may also contain limited amounts of belinite, calcium chloride orthosilicate, calcium ferrite (CF), periclas (MgO), alite (C_3S) and γ-C_2S. If the burning temperature is increased to 1370 °C and above, some of the alinite formed at lower temperatures converts to alite and at the same time the calcium chloroaluminate content is increased [Tsuchida et al., 1996].

Table 2 The main phases of alinite clinker [Odler, 2000]

	wt%
Alinite ($Ca_{10}Mg_{0.8}[(SiO_4)_{3.4}(AlO_4)_{0.6}O_2Cl$)	55-65
Belite ($2CaO.SiO_2$)	25-35
Calcium Chloro Aluminate ($11CaO.7Al_2O_3.CaCl_2$)	3-5
Dicalcium Ferrite ($2CaO.Fe_2O_3$)	3-5
Alite ($3CaO.SiO_2$)	5-7
Free Calcium Oxide (Free CaO)	<0.5

2.3.2 Chemical Composition of Alinite Phase

Alinite is a calcium oxy-chloro-aluminosilicate that is related to alite, the main constituent of Portland cement. Whereas in alite ($3CaO.SiO_2$), the main phase of Portland cement, the Ca^{2+} cations are balanced by SiO_4^{4-} and O^{2-} anions, the structure of alinite consists of Ca^{2+} and Mg^{2+} cations balanced by SiO_4^{4-}, AlO_4^{5-}, O^{2-} and Cl^- anions. Crystallographic studies have revealed that the main feature of alinite is the peculiar position of the chlorine atoms surrounded by eight calcium ions [Noudelman and Gadaev, 1986].

There are many suggested chemical formulas for alinite by different investigators [Odler, 2000]. Simply, the formula is $Ca_{11}[3(SiO_4).(AlO_4).O_2.Cl]$. In reality alinite may be stable only if some Mg^{2+} is also present in the crystalline lattice, substituting for Ca^{2+}. The proportions of SiO_4/AlO_4 in alinite are not constant and may vary between 3.35/0.65 and 3.45/0.55 [Noudelman et al., 1980]. Thus, the actual composition of alinite may be most accurately expressed by the following formula;

$$Ca_{10}Mg_{(1-x/2)}\square_{x/2}[(SiO_4)_{3/x}(AlO_4)_{1-x}O_2Cl] \quad (2)$$

where $0.35<x<0.45$ and □ refers to a lattice vacancy.

The crystalline lattice of alinite may accommodate limited amounts of additional ions, such as Fe^{3+}, P^{5+}, Ti^{4+}, Na^{+}, and K^{+} [Noudelman et al., 1980]. At least four modifications of alinite have been identified and designated as α, ά, β and γ [Noudelman and Gadaev, 1986].

Because of its solid solution type structure, alinite is remarkably tolerant to various impurities. Thus, coupled with its settling property alinite is suited for waste recycling and utilization Alinite may be synthesized using a starting mix containing $CaCO_3$, SiO_2, Al_2O_3, MgO and $CaCl_2$ by burning it at 1000-1200°C. At this temperature the rate of alinite formation exceeds that of tricalcium silicate (1400-1500°C) by about 7-8 times [Bikbaou, 1986]. At even higher temperatures the alinite converts to alite and this process is accompanied by a release of chlorine [Agarval et al., 1986].

2.3.3 Hydration of Alinite Cement

Alinite exhibits a higher hydraulic reactivity than alite phase. Table 3 shows the degree of hydration of the phases.

Table 3 Degree of hydrations of alinite cement [Odler, 2000]

Hydration time	**Degree of hydration (%)**		
	Alite	**Alinite - 1**	**Alinite - 2**
15 min	-	-	9
1 h	10	22	-
6 h	15	64	36
12 h	20	70	-
1 day	25	80	43
3 days	40	85	53
28 days	-	-	62

The hydration of alinite takes place without any distinction of induction period [Boikova et al., 1986]. A single exothermic peak is formed about 60-120 min after mixing and the hydration of alinite is significantly accelerated by the presence of free chlorine ions in the liquid phase [Neubauer and Pöllman, 1994].

The hydration products of alinite cement are as follows [Odler, 2000]:

- Similar to Portland cement C-S-H and CH phases produced from alinite and belite phases.

- Friedel's Salt ($C_3A.CaCl_2.10H_2O$) phase is formed in the hydration of calcium aluminochloride and also the ferrite phase resulting in substitution of Al^{3+} by Fe^{3+}.

- The monosulfate group, also known as AFm phase, is represented as $C_4A\overline{S}H_{12}$, $C_4(A,F)\overline{S}H_{12}$ $C_3A.C\overline{S}.H_{12}$. AFm stands for Al-Fe mono, in which one mole of $C\overline{S}$ is present [Ramachandran et al., 2002]. AFm phase is similar but not identical to

Friedel's salt since in it up to 15 mol% of $CaCl_2$ is replaced by $Ca(OH)_2$ and $CaCO_3$. [Neubauer and Pöllman, 1994]

- If calcium sulfate is interground with alinite clinker or in other words in mixes with gypsum, an AFt phase $C_6(A,F)S_3H_{32}$ may be formed. Ettringite belongs to AFt phase. It converts to monosulfate in the latter course of hydration. [Odler, 2000]

- Other phases including CAH_{10} and C_3AH_6 that may be present at small amounts.

The alinite cement has high early strength properties. Gypsum addition is reported to intensify strength development rather than principally functioning as a regulator of set [Hewlett, 2004].

Chlorine in alinite clinker becomes bound with the Friedel's salt phase ($C_3A.CaCl_2.10H_2O$) [Noudelman et al., 1980]. C-S-H phase may accommodate up to 3.5% Chlorine ions by adsorption [Odler, 2000].

2.4 Raw Materials for Portland Cement

For traditional Portland cement clinker the main raw materials are limestone, sand, shale, clay and iron ore. The main material, limestone, is usually mined on site while the other minor materials may be mined either on site or in nearby quarries. Another source of raw materials is industrial by-products. The use of by-product materials to replace natural raw materials is a key element in achieving sustainable development.

2.5 Raw Meal Optimization

Raw meal design of the clinker defines the specific ratios and module that relate oxide compositions to one another. Raw mix optimization modules enable to control the short term fluctuations to the target values such as the proper C_3S and C_2S values, etc. by optimizing and controlling the raw meal material proportions in the raw meal feed [Duda, 1985]. By some mathematical models, the quality deviations

in the clinker can be foreseen. This permits implementive predictive actions rather than reactive ones.

Mainly, there are three types of raw meal modules for clinker [Duda, 1985].

Lime Saturation Factor (LSF) = $CaO / (2.8SiO_2 + 1.2Al_2O_3 + 0.65Fe_2O_3)$

Silica Ratio (SR) = $SiO_2 / (Al_2O_3 + Fe_2O_3)$

Alumina Ratio (AR) = Al_2O_3 / Fe_2O_3

LSF largely governs the ratio of alite to belite and also shows whether the clinker is likely to contain an unacceptable proportion of free lime, a value of 1.0 or above indicating that the latter will be present at equilibrium at the clinkering temperature and thus liable to persist in the product. In practice values up to 1.02 may be acceptable; typical values for modern clinkers are 0.92-0.98. The higher the LSF, the better strength of cement, but the more difficult it becomes to burn the raw mix [UN Habitat, 1994]. A modification of LSF formula, intended to allow magnesium substitution in alite, replaces CaO by (CaO+0.75MgO) for MgO $\leq$2% or by (CaO+1.5) for MgO>2% [Sharma et al., 2004].

The SR governs the proportion of silicate phases in the clinker and increase in SR lowers the proportion of liquid at any given temperature in the kiln, thus makes the clinker more difficult to burn [Kuleli, 2009]. SR is usually between 2.0 and 3.0.

The AR governs the ratio of aluminate to ferrite phases and determines the liquid formed and affects the clinker properties. [Taylor, 1990]

For alinite clinker, due to the high Cl- content a modification of LSF is given as follows [Ftikos et al., 1993]:

LSF = $100(CaO-0.789Cl) / (2.8SiO_2 + 1.2Al_2O_3 + 0.65Fe_2O_3)$

CHAPTER 3

EXPERIMENTAL STUDY

3.1 General

Alinite cement was produced by using soda solid waste at different burning schemes. The raw meal is burned either in a platinum crucible or on refractory. After burning the raw meal, the phases of the clinker are detected by X-Ray Diffractometer. The chemical composition is defined by X-Ray Fluorescence (XRF) method. For certain samples, 28 day compressive strength values was measured and SEM images were observed. All the tests were performed at the research and development laboratories of Turkish Cement Manufacturers' Association.

3.2 Raw Mix Proportions

The main raw materials for alinite cement are soda solid waste, clay and iron ore in minor amounts. Soda solid waste or soda sludge is the by-product of the Solvay process. The raw mix of alinite clinker does not include any natural limestone from quarry, in order to maximize the soda waste usage and obtain low energy cement. Similar to the Portland cement, raw mix for alinite cement also contain clay and iron ore. These constituents are vital for liquid phase formation by clinkerization and by lowering the burning temperature. Chemical analyses were conducted by Atomic

Absorption Spectroscopy (AAS). Loss on ignition and Cl^- amounts were detected by wet chemical analyses by EN 196-2.

The large amount of Cl^- content of the soda waste is a key factor by deciding the attempt of producing alinite clinker, since alinite phase requires Cl^- in its lattice stucture. The related mix proportions have been found by the proper mixing modules given in Table 4. One mix was prepared and all the different burning trials were performed by the same raw mix.

Table 4 Mixing modules of alinite raw feed

Lime Staruration Factor (LSF)	76.12
Silica Module (SM)	2.60
Alumina Module (AM)	1.93

In the case of high chlorine content the modified LSF is found as 69.31.

The mixing modules were calculated by the assumption of x part of soda solid waste, y parts of clay and 1 part of iron ore by weight. [Duda, 1985] In order to obtain the given modules the recipe for the raw mix shown in Table 5 was utilized.

Table 5 Recipe of the raw mix

	wt%
Soda Solid Waste	73.5
Clay	26.3
Iron ore	0.2

Solid waste from Mersin Soda plant was wet and in agglomerated form as received. There was an option to reduce the chlorine content of the waste from 6 wt% down to 1 wt%. However, for the case of alinite clinker chlorine is required to form the alinite phase properly. Therefore, the waste with high chlorine content of about 6 wt% was utilized throughout this study. Solid soda waste was first dried and ground leading to a suitable powder form approximately of 90 μm.

3.3 Burning Scheme

The furnace used in the burning experiments is Protherm brand, suitable for clinker burning up to 1450°C. In order to observe the effects of different burning temperatures and duration on alinite clinker formation, 11 different burning regimes were selected. The burning regimes are presented along with the sample codes in Table 6. The samples are coded as "A + maximum burning temperature + burning duration". All the samples had the same raw mix. Burning durations were kept higher than an ordinary Portland clinker to ensure the complete burning.

Table 6 The burning regimes of the raw feed and the labeling of the samples

Sample Code	Burning Temperature (°C)	Duration (min)
A1050-60	1050	60
A1050-90	1050	90
A1100-60	1100	60
A1100-90	1100	90
A1150-60	1150	60
A1150-90	1150	90
A1200-60	1200	60
A1200-90	1200	90
A1200-180	1200	180
A1350-10	1200+1350	180+10
A1450-10	1450	10

The heating steps of the samples were the same up to a certain temperature. The samples were first heated to 700°C at a heating rate of 50°C/min. Then they were kept at this temperature for 10 minutes. After that, they were heated to 1000°C at 30°C/min and were kept at this temperature for 5 min. From this point, the heating was different for each sample. The samples were heated up to their maximum burning temperature stated and were kept at this temperature for a certain time indicated as duration in Table 6. By this way, all the parameters were kept constant and only the effects of temperature and time were observed. For the sample A1350-10 different burning scheme was performed. The sample was heated to 1200°C for a duration of 180 min. and then it was heated to 1350°C at 30°C/min and was kept at this temperature for a duration of 10 min.

For the chemical and mineralogical analyses the raw feed was burned in small platinum crucibles. The samples namely A1200-60, A1200-180, A1350-10 and A1450-10 needed to be burned in relatively larger quantities for compressive strength analyses. In order to obtain a uniform burning in the furnace the raw feed was mixed with water and was given small rode shape.The rods were placed on a refractory plate. A thin platinum plate was placed between the layers of them in order to prevent sticking of the clinker to the refractory plate. After certain durations at the maximum temperature, the clinkers was taken out of furnace and cooled at ambient temperature.

3.4 Tests on Alinite Clinker

Chemical and mineralogical analyses of 11 clinker specimens burned in small platinum crucibles were done according to the standard test method EN 196-2. X-Ray Diffraction (XRD) analyses were performed. Four of the samples namely A1200-60, A1200-180, A1350-10 and A1450-10 were produced in larger quantities in order to determine 28 day compressive strength according to the standard test method EN 196-1 with a 0.4 water/cement ratio. In addition to the chemical analyses, physical properties such as density and specific surface area and compressive strength were measured.

3.4.1 Chemical Analysis

After burning, as the first step free CaO amount were detected following the test method described in EN 196-2. The loss on ignition (LOI) tests were done in a furnace at 975°C. The major oxides of the clinker samples were detected XRF. The samples were prepared in both powder and glass bead specimen form since the volatile contents like alkalis and chlorine cannot be detected as melted. The Sulfur oxide and Chlorine contents were determined according to the standard test method of EN 196-2.

3.4.2 X-Ray Diffraction

X-Rays are an electromagnetic radiation of short wavelength and can be produced by sudden deceleration of rapidly moving electrons at a target material [Ladd and Palmer, 2003]. The X-Ray Diffraction (XRD) pattern of a pure substance can be considered as a fingerprint of the substance. The powder diffraction method is thus ideally suited for characterization and identification of polycrystalline phases.

XRD is the most reliable and convenient tool for ascertaining the formation of alinite phase in clinker. XRD analyses were done with a Philips brand device. The entire specimens were tested with Cu Kα radiation in 2θ of 5-60° with 2° interval. The phases present in the samples were detected.

3.4.3 Density and Specific Surface Area

Density of both the raw materials and resultant clinker specimens were determined by a digital pycnometer. The main function of the device is finding the volume of the powder materials in a closed box with a compressed gas having a certain pressure, then dividing the weight of the powder to the volume.

Specific surface area of a powder material means the total surface area of a unit weight of powder. This property is determined by Blaine apparatus in accord with the EN196-6 standard test method. The fundamental principle of the device is

squeezing the powder specimen and measuring the time for the air passing through the sample.

Density and specific surface area of the samples A1200-60, A1200-180 and A1200-60 with gypsum addition were determined.

3.4.4 Powder Particle Size Distribution by Laser Diffraction

Laser diffraction techniques are one of the most common diagnostic for multi particle size analysis. The beam from a laser, typically a several mW He-Ne model is spatially filtered, expanded and collimated to several millimeter diameters. Light scattered particles in the probe beam which passes though the aperture of the receiving lens is directed to off axis points on the observation or detection plane [Hirleman, 1994].

Particle size distribution for the raw mix was determined by a laser diffractogram and given in Appendix A.

3.4.5 Compressive Strength

The compressive strength is one of the most important parameters of cement quality. According to TS EN 196-1 standard method, with regard to the type of the cement 2-7-28 day compressive strength values should be determined. The test method suggests using a water/cement ratio of 0.5 and standard sand. The mortars being cured in water at a temperature of 20 ˚C then subjected to compressive strength test. The surface dimensions of the crushing plate are 40*40mm, so the area is 40*40=1600 mm^2. Compressive strength of the samples was calculated as ultimate force divided by the surface area according to the expression given below [EN 196-1, 2009]:

$$\sigma = P/A \quad (3)$$

σ: Compressive strength (MPa)

F: Force (N)

A: Area (mm^2)

Compressive strength of the clinkers A1200-60, A1200-180, A1350-10 and A1450 were determined. The water/cement ratio of the mortars were kept 0.4 in order to obtain higher compressive strength values. After 28 days the specimens were subjected to compressive load.

A1200-60 was burned at 1200°C for 60 min whereas A1200-180 was burned at the same temperature for 180 min. The effect of burning duration on compressive strength was clarified. Moreover, A1200-60 was molded both by 5% gypsum addition and without any addition. The effect of gypsum additive on the compressive strength was also determined.

3.4.6 Scanning Electron Microscope

Scanning electron microscopy (SEM) is a widely used tool for imagining and analyzing micro and macro structure of bulk specimens. The principle of SEM is that the electrons from a thermionic, Schottky or field-emission cathode are accelerated through a voltage difference between cathode and anode that may be as low as 0.1 keV or as high as 50 keV. The smallest beam cross section at the gun is demagnified by two or three stage electron lens system. A diffraction coil system in front of the final lens field scans the electron probe with an electron beam of a separate cathode-ray tube (CRT). The intensity of the CRT is modulated by one of the signals recorded to form an image [Reimer, 1998].

SEM employed in this study is LEO 435 VP. For samples A1200-60 and A1200-180 SEM examination were done in order to observe the effects of burning duration on microstructure. Since the SEM uses electrons to produce an image, the sample preparation step includes making the sample electrically conductive by covering the material with a thin layer of conductive metal. Samples were prepared by the sputter coater device. The SEM images of A1200-60 were taken with 752X, 1.76KX and 3.22KX magnifications, whereas A1200-180 was subjected to 750X, 1.75KX and 3.20KX magnifications.

CHAPTER 4

RESULTS AND DISCUSSION

4.1 Raw Materials and Raw Mix Properties

Chemical compositions of the raw materials used in this study determined by atomic absorption spectroscopy are given in Table 7. Since the soda solid waste was wet as received from the Mersin Soda Plant the LOI value is high. Solid waste does not contain aluminum oxide. The Al_2O_3 requirement for the raw mix was met mainly by clay. The CaO content of the solid waste was high enough for clinker synthesis. Since the alinite phase includes Cl^- in its lattice structure, the large amount of Cl^- content of solid waste is also important.

The mineralogical analyses of raw miw revealed that the soda waste contains both $CaCO_3$ and $Ca(OH)_2$ as presented in Figure 1.

Table 7 Chemical analyses of the solid soda waste and raw materials

Composition (wt %)	Soda Solid Waste	Clay	Iron Ore	Raw Mix
LOI	34.59	10.11	9.39	28.11
SiO_2	1.33	57.13	39.46	16.09
Al_2O_3	0.00	15.45	2.26	4.07
Fe_2O_3	0.72	5.74	47.56	2.11
CaO	50.90	5.97	0.75	38.99
MgO	1.81	2.57	0.20	2.01
SO_3	3.02	0.00	0.09	2.22
Na_2O	1.55	0.89	0.10	1.37
K_2O	0.07	2.14	0.19	0.62
Cl^-	6.01	0.00	0.00	4.42
Total	100.00	100.00	100.00	100.00

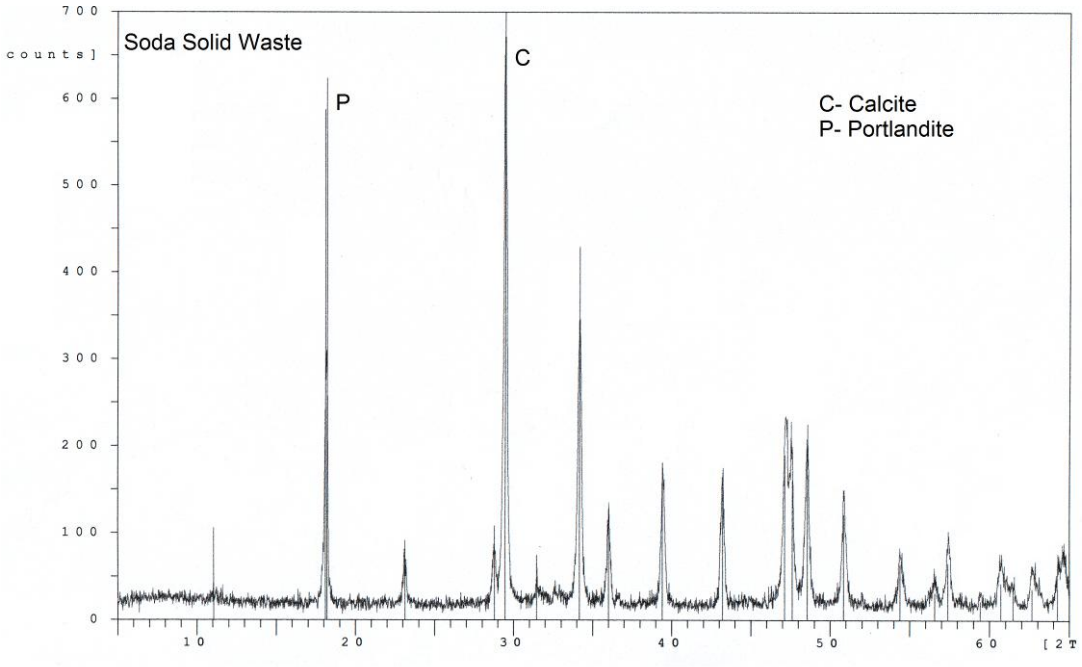

Figure 1 XRD pattern of solid soda waste

4.2 Alinite Clinker Properties

The results of alinite clinker are presented in the subtitles as chemical properties, mineralogical properties, physical and mechanical properties, and SEM.

4.2.1 Chemical Properties

The results of the chemical analyses of alinite specimens are given in Table 8. Since the raw mix for all clinker specimens is the same, the chemical analyses results do not show much deviation. The main remarkable difference between the specimens is in loss on ignition. Increasing the burning temperature and duration caused a decrease in the values of LOI. LOI terms as the loss of the water and CO_2 of the clinker by heat [Taylor, 1990]. Water at these high temperature is lost completely. The reason of that difference is that at higher burning temperatures the conversion of the $CaCO_3$ to CaO increases and more CO_2 comes out. After the clinker is taken out of the furnace and cooled to room temperature, LOI test were conducted and lower LOI values are obtained with the samples burned at higher temperatures. In other words, this revelas more complete burning at higher temperatures. Moreover the free lime decreased by increasing burning temperature and time. These data indicate whether the burning is fully completed or not. Free lime and LOI obtained at temperature of 1200 ºC can be taken as complete burning. Furthermore, as seen in Table 8, as the maximum duration temperature increased, the oxide compounds by weight percent were increased. Due to the decrease in the loss on ignition and free lime values. The decrease in Cl^- contents with increasing temperature is attributed to its volatility.

Unlike Portland cement clinker, alinite clinker includes large amount of Sulfur tri oxide (SO_3). The SO_3 is located in the Calcium Chloride Silicate Sulfate [$Ca_{10}(SiO_4)_3(SO_4)_3Cl_2$] phase which also contains Cl^- ions. Since the Cl^- ions are not free in the lattice structure their harmful effects are minimized [Odler, 2000].

Table 8 Chemical analyses results of the specimens

Composition Weight%	**A1050-60**	**A1050-90**	**A1100-60**	**A1100-90**	**A1150-60**	**A1150-90**	**A1200-60**	**A1200-90**	**A1200-180**
LOI	4.82	4.41	4.19	3.08	1.93	1.82	1.26	0.39	0.18
Free CaO	2.39	2.30	1.96	1.83	1.57	1.51	1.14	1.05	0.12
SiO_2	19.91	20.39	20.30	20.79	20.97	21.42	21.43	21.72	23.60
Al_2O_3	5.90	5.94	5.96	6.13	6.13	6.23	6.32	6.50	6.86
Fe_2O_3	3.39	3.41	3.31	3.36	3.32	3.40	3.47	3.51	3.66
CaO	50.60	51.21	52.56	53.52	55.12	55.56	55.48	56.74	57.01
MgO	2.75	2.79	2.82	2.87	2.90	2.96	2.99	3.01	3.09
SO_3	3.44	3.48	3.21	3.32	3.35	3.28	3.53	3.41	3.14
Na_2O	1.33	1.15	1.18	0.93	0.74	0.56	0.51	0.42	0.28
K_2O	0.35	0.28	0.28	0.15	0.11	0.04	0.07	0.04	0.03
Cl^-	5.12	4.64	4.60	4.02	3.86	3.20	3.80	3.21	2.03
Total	**100.00**	**100.00**	**100.00**	**100.00**	**100.00**	**100.00**	**100.00**	**100.00**	**100.00**

4.2.2 Mineralogical Properties

In the XRD patterm of all alinite clinker samples alinite phase [$Ca_{10}Mg_{0.8}[(SiO_4)_{3.4}(AlO_4)_{0.6}O_2Cl$] was clearly detected. A typical XRD pattern of A1050-60 is illustrated in Figure 2. XRD results of other samples are presented in Appendix-B. For groups starting with samples A1050-60 to A1200-90, a distinct difference is not observed, that is, crystal formations are similar. At temperatures above 1200 ºC Belinite [$Ca_8Mg[(SiO_4)_4Cl_2$] was not observed and alinite decreased gradually since the intensities of related peaks decreased. Up to the burning temperature of 1200 ºC the intensities of the alinite peaks are above 800 whereas at 1200 ºC it is between 600 and 800. Moreover by burning at 1350 and 1450 ºC the intenties of the alinite peaks are between 400 and 600. At 1450ºC Calcium Aluminochloride [$C_{11}A_7CaCl_2$] and Free Lime [CaO] decreased whereas Ferrite [C_4AF] increased.

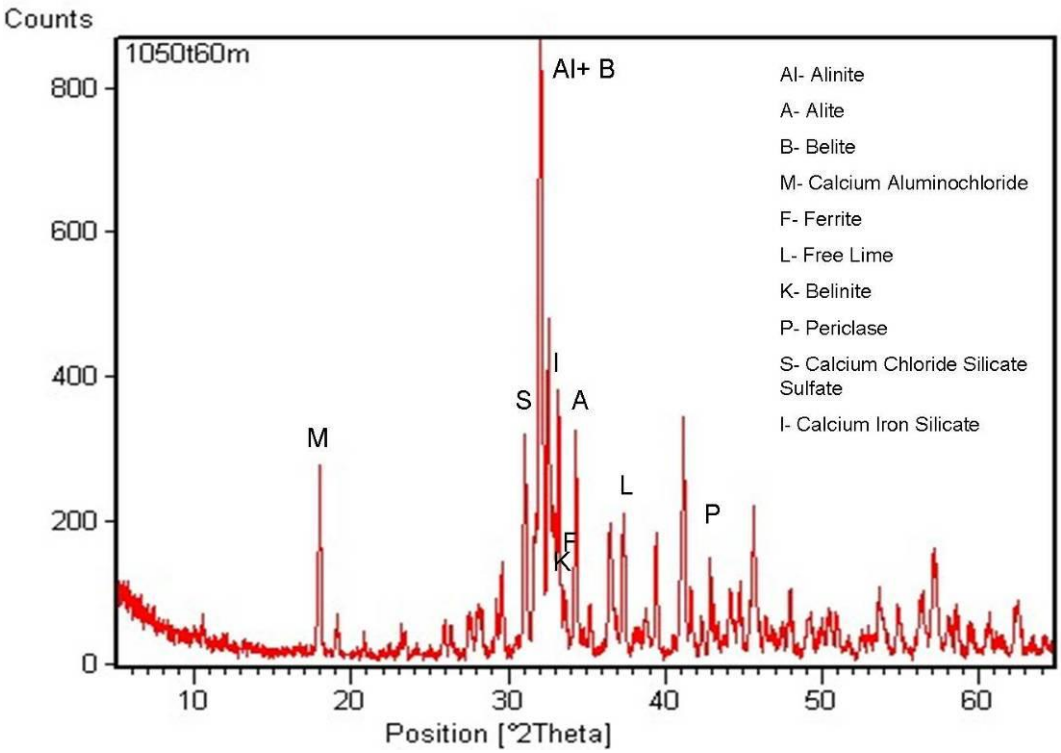

Figure 2 XRD pattern of A1050-60

A1050-60 **Temperature:** 1050ºC **Duration:** 60 min

Alinite [$Ca_{10}Mg_{0.8}[(SiO_4)_{3.4}(AlO_4)_{0.6}O_2Cl]$]
Belite [C_2S]
Calcium Aluminochloride [$C_{11}A_7CaCl_2$]
Ferrite [C_4AF]
Free Lime [CaO]
Belinite [$Ca_8Mg[(SiO_4)_4Cl_2]$]
Periclase [MgO]
Calcium Chloride Silicate Sulfate [$Ca_{10}(SiO_4)_3(SO_4)_3Cl_2$]
Calcium Iron Silicate [$Ca_3Fe_2(SiO_4)_3$]
Alite [C_3S]

4.2.3 Physical and Mechanical Properties

The results of the physical analyses are given in Table 9. A1200-60, A1200-180, A1350-10 and A1450-10 burned in wet rod shape were cast with a w/c ratio of 0.4. For the samples A1200-60 and A1200-180 the results reveal that when burning duration is increased from 60 to 180 min no significant distinct difference in compressive strength is obtained.

Table 9 Physical and mechanical analyses results of the alinite specimens

		A1200-60	**A1200-60***	**A1200-180**
Density	(g/cm^3)	3.20	3.20	3.20
Specific Surface - Blaine	(cm^2/g)	4310	4300	4300
w/c		0.4	0.4	0.4
28 day Compressive Strength	(MPa)	4.4	26.6	4.8

* The specimen cast with 5% gypsum addition

For A1200-60 and A1200-180 average of six individual values is given, whereas for A1200-60* due to the limited amount of sample, average of four individual values is given. In accord with a a study from literature 28 day compressive strength result of alinite cement is 35.3 MPa with a specific surface of 5550 cm^2/g and tested as IS 431 [Singh, 2008]. The reason of the difference in the compressive strength is that, for the samples in the literature was produced from limestone and some addition. However, in this study instead of limestone, soda solid waste was used as the main raw material. Furthermore, the specific surface area of the samples in the study of Singh, 2008 are higher resulting in higher compressive strength.

When the sample A1200-60 was cast with 5% gypsum addition a noticeable increase in 28 day compressive strength value was observed. This was attributed to the ettringite formation by gypsum addition [Odler, 2000]. In order to verify this, two different cement pastes of A1200-60 with gypsum addition and without gypsum addition were prepared and XRD patterns of hardened pastes at 7 days old were detected and presented in Figures 3 and 4.

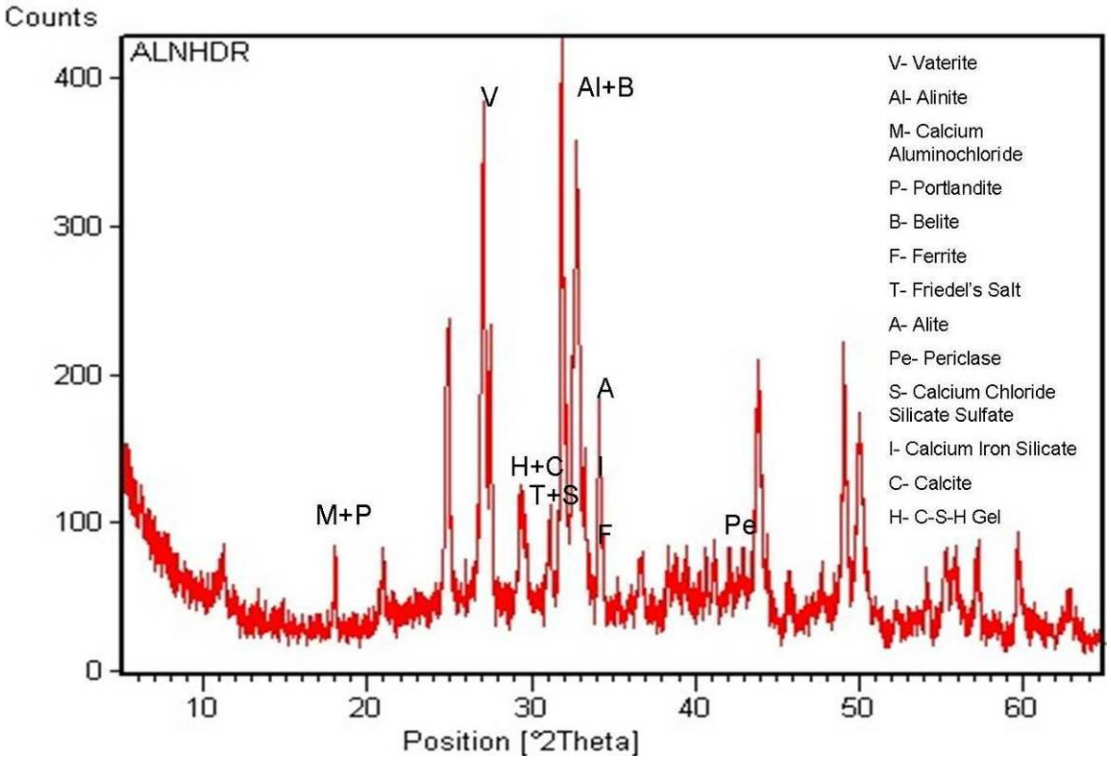

Figure 3 XRD pattern of hardened A1200-60 PASTE 7days old

A1200-60 Paste

(Cast without standart sand)

Friedel's Salt [$3CaO.Al_2O_3.CaCl_2.10H_2O$],

Portlandite [$Ca(OH)_2$]

C-S-H gel

Alinite [$Ca_{10}Mg_{0.8}[(SiO_4)_{3.4}(AlO_4)_{0.6}O_2Cl]$]

Belite [C_2S]

Calcium Aluminochloride [$C_{11}A_7CaCl_2$]

Ferrite [C_4AF]

Periclase [MgO]

Calcium Chloride Silicate Sulfate [$Ca_{10}(SiO_4)_3(SO_4)_3Cl_2$]

Calcium Iron Silicate [$Ca_3Fe_2(SiO_4)_3$]

Alite [C_3S]

Vaterite [$CaCO_3$]

Calcite [$CaCO_3$]

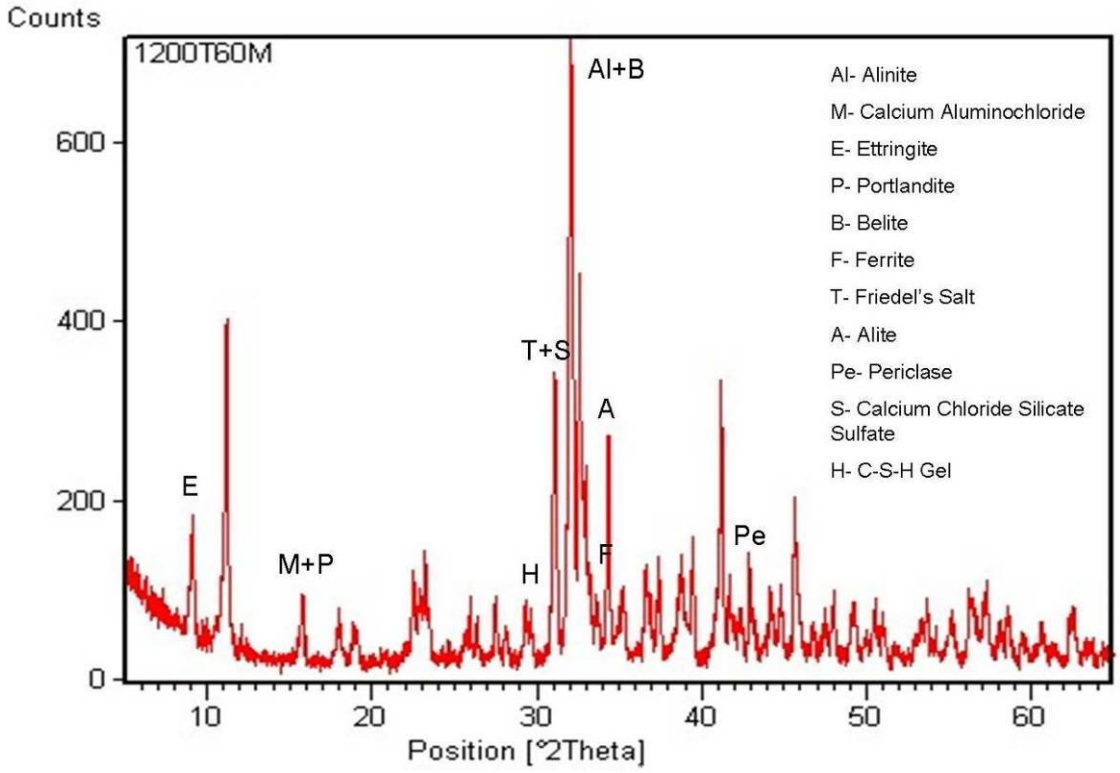

Figure 4 XRD pattern of hardened A1200-60 PASTE with Gypsum addition 7 days old

A1200-60* Paste with Gypsum addition

(Cast with gypsum [$CaSO_4.2H_2O$] addition)

Friedel's Salt [$3CaO.Al_2O_3.CaCl_2.10H_2O$]

Ettringite [$Ca_6Al_2(SO_4)_3(OH)_{12}.26H_2O$]

C-S-H gel

Portlandite [$Ca(OH)_2$]

Alinite [$Ca_{10}Mg_{0.8}[(SiO_4)_{3.4}(AlO_4)_{0.6}O_2Cl$]

Belite [C_2S]

Alite [C_3S]

Ferrite [C_4AF]

Periclase [MgO]

Calcium Aluminochloride [$C_{11}A_7CaCl_2$]

Calcium Chloride Silicate Sulfate [$Ca_{10}(SiO_4)_3(SO_4)_3Cl_2$]

For Hydrated phases A1200-60 paste and A1200-60* paste (with 5% gypsum addition), Friedel's Salt [$3CaO.Al_2O_3.CaCl_2.10H_2O$], Portlandite [$Ca(OH)_2$], C-S-H gel and other phases were observed. In A1200-60* cast with gypsum addition Ettringite [$Ca_6Al_2(SO_4)_3(OH)_{12}.26H_2O$] was detected. Moreover, A1200-60 paste showed Vaterite [$CaCO_3$]. Upon exposure to moist air, some reaction with water (hydration) and/or with carbon dioxide (carbonation) occured, called aeration [Hewlett, 2004]. Since this phase is not stable in ambient conditions, it is converted into Calcite [$CaCO_3$] which was also detected.

Samples A1350-10 and A1450-10 burned at higher temperatures (1350-1450°C) were melted in furnace. After they were taken out from furnace, they were dried, crushed and cast to determine the compressive strength. However, they did not show any hydraulic property. Alinite phases are dissolved at these temperatures and the XRD results show that the intensity of the characteristic alinite peaks decreased.

4.2.4 Scanning Electron Microscope

The crystal structures of specimens having different burning schemes are one of the key points to find out the effects of burning time. Two of the samples namely A1200-60 and A1200-180 were examined by SEM. The images with three magnifications are provided in Figures 5 and 6. As seen in Figure 5, A1200-60 shows little crystals of alinite, belite and other phases, whereas in Figure 6 A1200-180 shows relatively larger crystals. As the burning duration increased, alinite crystals were grown and the number of belite crystals increased. For both specimens few alite crystals have been detected. However, this did not affect the 28 day compressive strength presented in part 4.2.3.

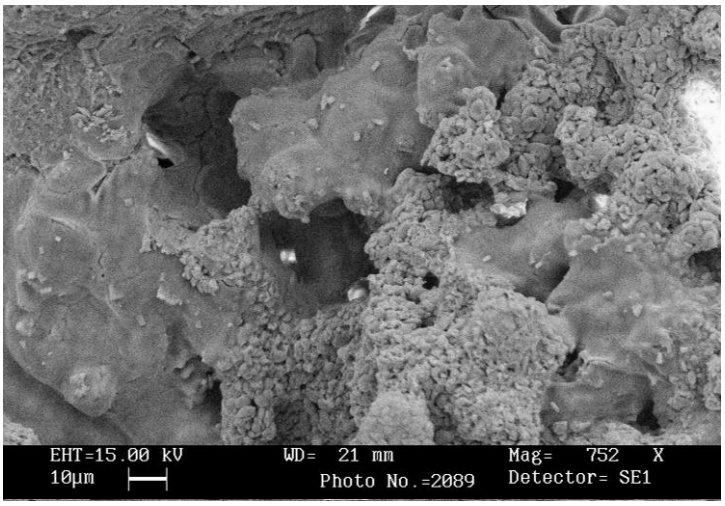

(A)

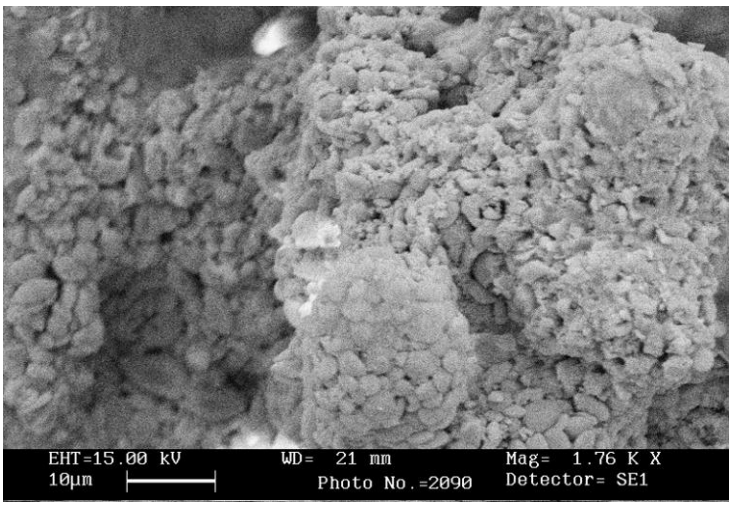

(B)

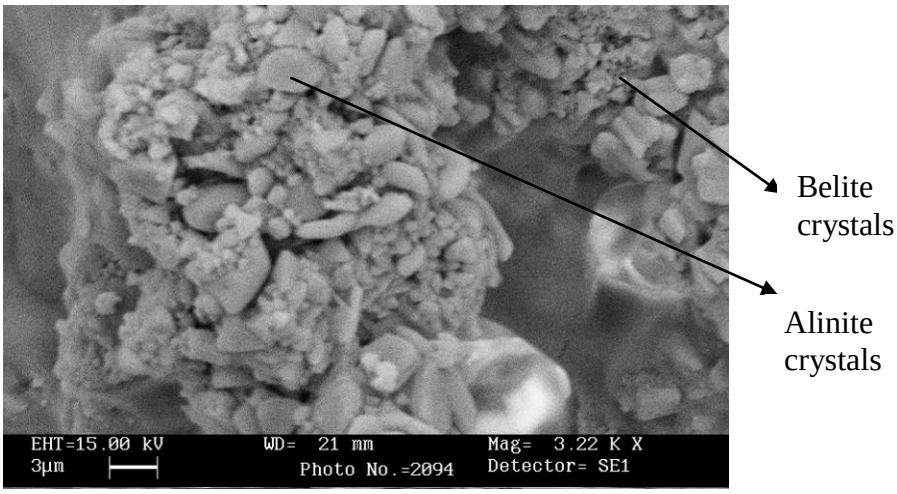

(C)

Figure 5 SEM images of sample A1200-60 burned at 1200°C with 60 minutes duration (A) 752 X (B) 1.76 K X (C) 3.22 K X magnification values

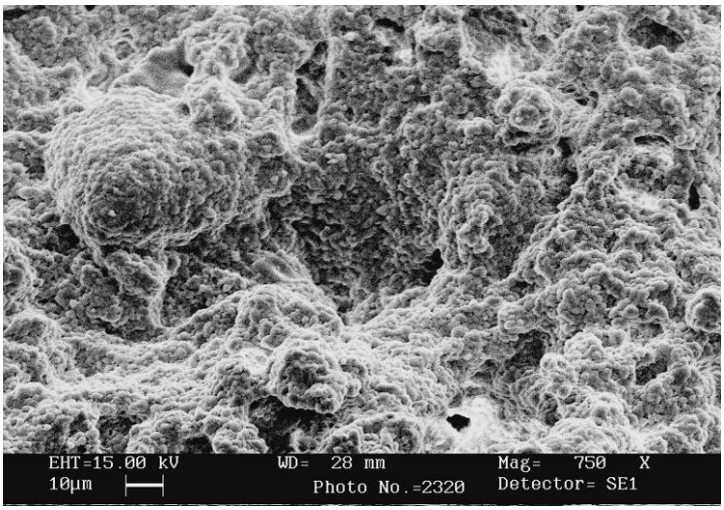

(A)

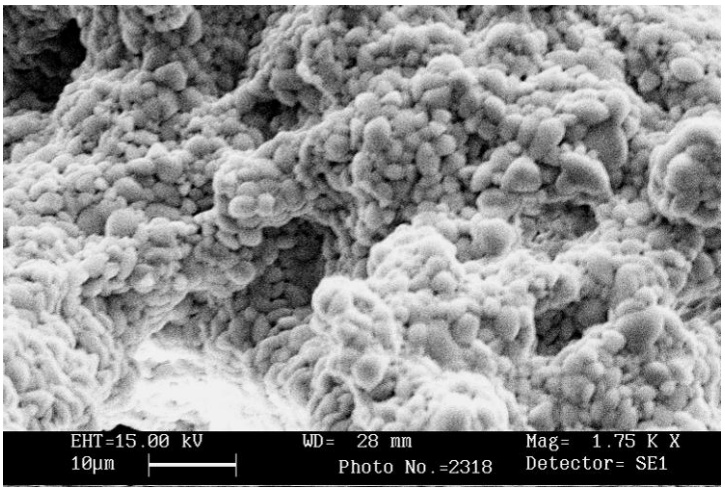

(B)

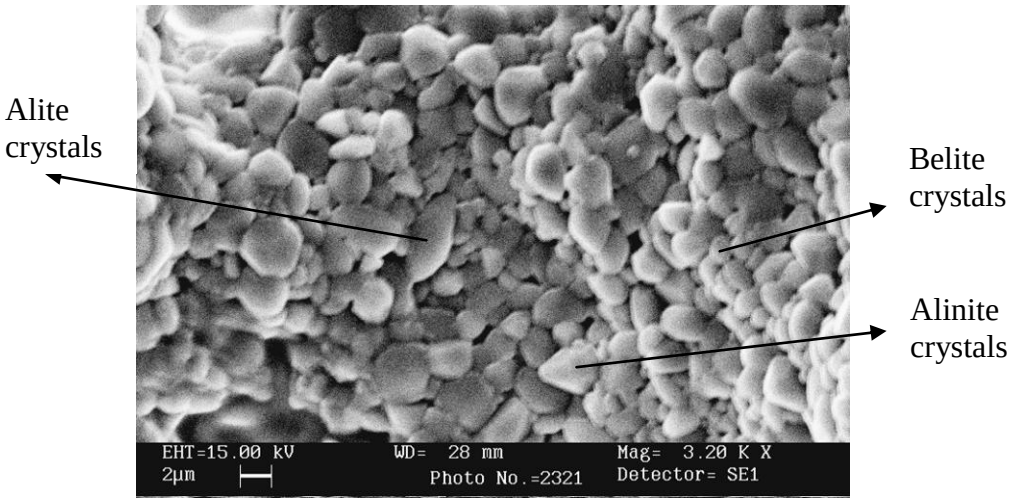

(C)

Figure 6 SEM images of sample A1200-180 burned at 1200°C with 180 minutes duration (A) 750 X (B) 1.75 K X (C) 3.20 K X magnification values

Phases shown in the SEM images were detected by EDS spectrum analyses. The certain EDS spectrum patterns for alite and belite phases are presented in Figure 7 and 8.

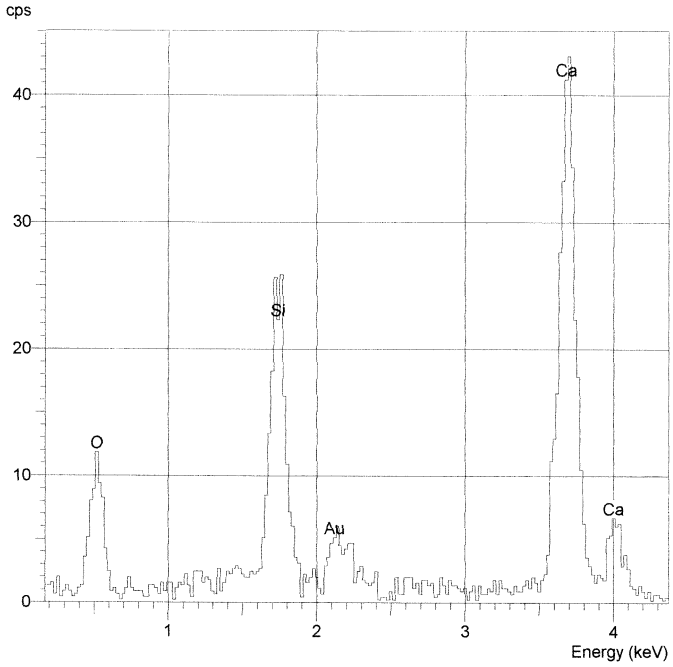

Figure 7 EDS Spectrum of alite phase of sample sample A1200-60

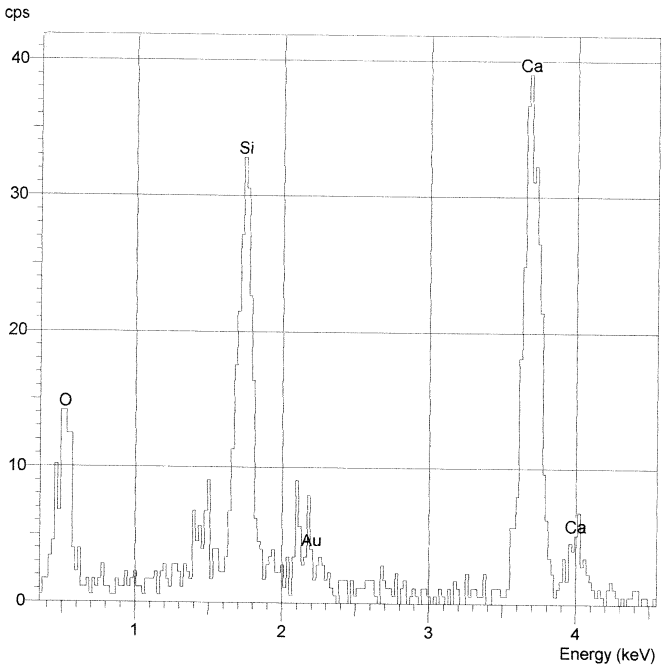

Figure 8 EDS Spectrum of belite phase of sample sample A1200-60

The alinite phase EDS patterns of this study and of another study from literature are presented in Figures 9 and 10. The similarity of the patterns ensure the formation of the alinite phase.

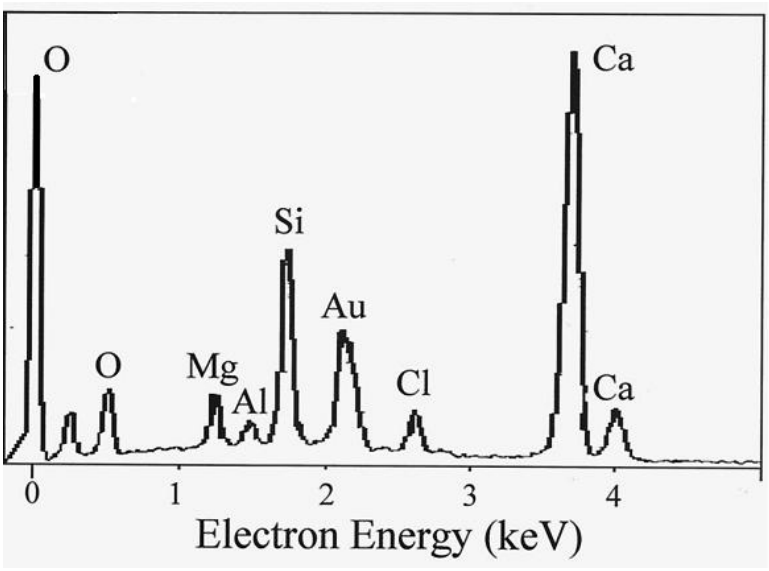

Figure 9 EDS spectrum of alinite particles calcined at 1300 °C [Kim, 2002]

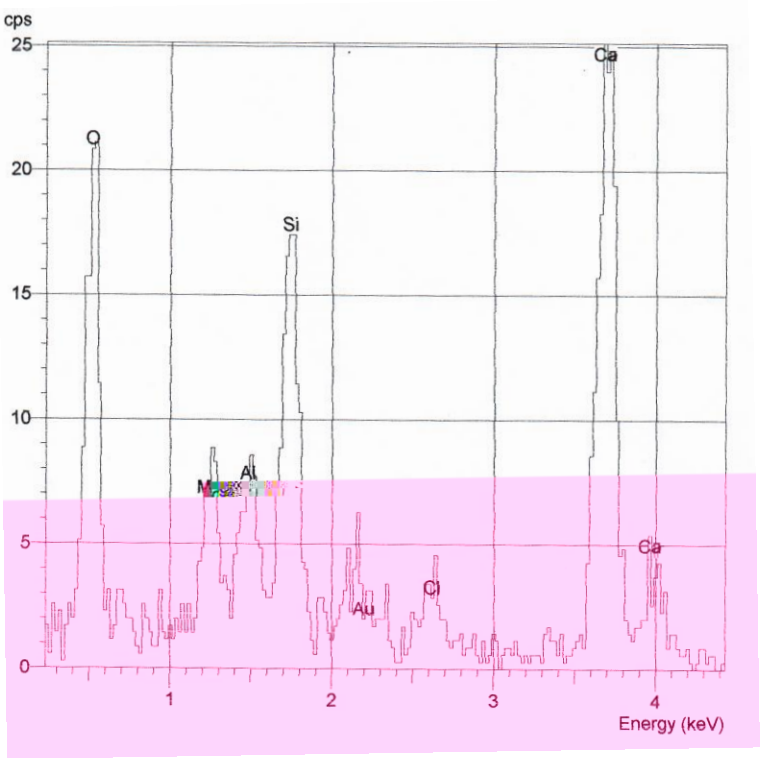

Figure 10 EDS spectrum of alinite phase of sample sample A1200-60

CHAPTER 5

CONCLUSIONS AND RECOMMENDATIONS

The thesis discusses an experimental program that works up synthesis of alinite cement from soda solid waste. The solid waste did not have a pretreatment such as washing and decreasing the chlorine content etc. According to the chemical analyses of the soda solid waste as received an optimum raw mix for clinker production is determined and a series of burning schemes were tried. The following conclusions can be drawn:

1. Alinite clinker was successfully synthesized with a burning temperature starting with 1050°C, up to 1200°C. Characteristic XRD pattern of alinite phase was obtained. Due to compressive strength and low free lime content, 1200°C was selected as optimum burning temperature.

2. Alinite formation decreased gradually at temperatures above 1200 ºC whereas belinite was not observed. Burning at 1450 ºC for 10 min results in complete melting of the clinker and gives no compressive strength after hydration. Burning at 1200 ºC for 180 min and 1350 ºC for 10 min also did not give hydration property. Optimum burning temperature for alinite clinker was detected as 1200 ºC.

3. Duration of burning did not change the mineralogical composition significantly. Keeping alinite clinker at maximum burning temperature for 60 and 90 min yielded similar results. Keeping alinite clinker at maximum burning temperature for 180 min for other than 60 min show growing crystals and more uniform structure. However, the compressive strength values did not change significantly.

4. Hydrated A1200-60 paste without gypsum addition and A1200-60* paste with gypsum addition have Friedel's Salt phase as the main hydration product. However, A1200-60* paste showed also certain Ettringite characteristic peaks. An increase in ultimate compressive strength was observed by gypsum addition due to the formation of Ettringite phase. Ettringite a type of AFt phase was detected clearly in XRD pattern.

5. In comparison with ordinary portland clinker, alinite clinker has threefold benefits in terms of economy, ecology and sustainability. First, portland clinker is manufactured around 1450 °C whereas the alinite clinker is obtained at 1200 °C. The 250 °C difference between burning temperatures gives the alinite cement its low energy characteristics. Considering the rotary kiln conditions and the amount of clinker to be burned, this reduction in burning temperature may give considerable energy savings in cement production. The second property of the alinite cement is that the raw meal of the clinker does not contain any limestone from quarry. In this study, alinite cement was produced from a raw mix including soda solid waste, clay and iron ore in minor amounts. Therefore, the use of natural limestone will be reduced resulting in saving the natural resources. Finally, CaO in the soda solid waste is both in the form of $Ca(OH)_2$ and $CaCO_3$, leading to less CO_2 emissions than using only limestone as the raw material.

Further study can be done in order to extend the study to change the raw mix proportions, compressive strength tests with different specific surface areas, water/ cement ratios and additions. Another important parameter for alinite clinker is the chlorine content and its deleterious effects to steel reinforcing bars. One important parameter is that, the amount of Cl^- in the alinite phase and free in the lattice. Therefore, durability issues could also be studied.

REFERENCES

1. Agarval, R.K., Paralkar, S.V., and Chatterjee, A.K., *Chloride Salts as Reaction Medium for Low Temperature Clinkerization – A Probe into Alinite Technology*, in Proceedings 8th ICCC, Rio de Janerio, Vol. 2, 1986.

2. Benstend, J., and Barnes, P. (editors), *Structure and Performance of Cements*, Elsevier Science Pub. Co. 2nd Ed., 1994.

3. Bikbaou, M.Y., *Formation, Crystal Chemistryand Properties of Alinite and Jasmundite*, in Proceedings 8th ICCC, Rio de Janerio, Vol. 2, 1986.

4. Boikova, A.I., Grishenko, L.V., and Domansky, A.I., *Hydration Activity of Chlorine Containing Phases*, in Proceedings 8th ICCC, Rio de Janerio, Vol. 3, 1986.

5. Bowen D.K., Tanner B.K., *High Resolution X-ray Diffractometry and Topography*, Taylor & Francis Ed., 2002.

6. Duda, Walter H., *Cement Data Book*, Vol.1, Bauverlag, Wiesbaden Berlin, 3rd Ed., 1985.

7. EN 196-1, *Methods of Testing Cement - Part 1: Determination of Strength*, 2009.

8. EN 196-2, *Methods of Testing Cement- Part 2: Chemical Analysis of Cement*, 2010.

9. EN 196-6, *Methods of Testing Cement - Part 6: Determination of Fineness*, 2000.

10. European Industry Chemical Council, *Soda Process Bref for Soda Ash*, Issue No:3, ESAPA, March 2004.

11. Ftikos, C.H., Philipou, T.H., Marinos, J., *A study of the Effect of Some Factors Influencing Alinite Clinker Formation*, Cement and Concrete Research 23, 1993.

12. Gür, N., Aktaş, Y., Civaş, A., *Utilization of Solid Waste of Soda Ash Plant as a Mineral Additive in Cement*, Cement and Concrete World, 2010.

13. Hewlett Peter C., *Lea's Chemistry of Cement and Concrete*, 4th Edition, Elsevier Science &Technology Books, 2004.

14. Hirleman E.D., *Particle Sizing by Optical Nonimaging Techniques Liquid Particle Size Detection Techniques*, American Society for Testing and Materials, 1994.

15. Iancu, O., Manea, A., Cojoc, D., *Advanced Topics in Optoelectronics, Microelectronics and Nanotechnologies*, Optoelectronics Research Center, Romaina, 2002.

16. Ji, L.,Ren, X., and Su, H., *Effect of Chloride on Hydration Properties of Alinite Cement*, in proceeding 10th ICCC, Goteborg, 1997.

17. Kim, Young-Min et al., *Synthesis and Hydration Characteristics of Alinite Cement*, J. Am. Ceramic Soc. 85 , Korea, 2002.

18. Kuleli, Ö., *Çimento Mühendisliği El Kitabı*, Türkiye Çimento Müstahsilleri Birliği, 2009.

19. Ladd, M., Palmer, R., *Structure Determination by X-Ray Crystallography*, Kluwer Academic/Plenum Publishers, 2003.

20. Locher, F.V., *Low Energy Clinker*, in Proceedings 8th ICCC, Vol. 1, Rio de Janerio, 1986,

21. Neubauer, J., and Pöllmann, H., *Alinite- Chemical Composition, Solid Solution and Hydration Behaviour*, Cement and Concrete Research 24, 1994.

22. Noudelman, B.I., and Gadaev, A.I., *Physico-chemical Aspects of the Crystallization of Chlorsilicates after Clinkerization at Lower Temperatures in Melted Salts*, in Proceedings 8th ICCC, Vol. 2, Rio de Janerio, 1986.

23. Noudelman, B. et al., *Structure and Properties of Alinite and Alinite Cement*, in Proceedings 7th ICCC, Vol. 3, Paris, 1980.

24. Odler, I., *Special Inorganic Cements*, Modern Concrete Technology, 2000.

25. Pradip, A., and Kapur, P.C., *Production and Properties of Alinite Cements From Steel Plant Waste*, Cement and Concrete Research 20, 1990.

26. Pradip, A., and Kapur, P.C., *Manufacture of Eco-friendly and Energy-efficient Alinite Cements from Flyashes and other Bulk Wastes*, Resources Processing, Vol. 51, No.1, 2004.

27. Ramachandran, V.S., Paroli, Ralph M., Beaudoin, James J., *Handbook of Thermal Analysis of Construction Materials*, Delgado, Ana H., William Andrew Publishing/Noyes, 2002.

28. Reimer, L., *Scanning Electron Microscopy – Physics of Image Formation and Microanalysis*, Springer 2nd Ed., 1998.

29. Roebuck C.M., *Excel HSC Chemistry*, 2004.

30. Sharma K.M., Sharma, P.S., Yadav D., *Problems and Prospects of Use of Soda Ash Sludge in Cement Industry*, Elsevier, 2004.

31. Singh et al., *Waste Management*, Volume 28, Issue 8, 2008.

32. Taylor, H.F.W., *Cement Chemistry*, Academic Press London, 1990.

33. Tsuchida, Y. et al., *Hydration and Characterization of Alinite Rich Clinker Burnt at Different Temperatures*, Journal of Research of the Chichibu Onoda Cement Corporation, 1996.

34. United Nations Centre for Human Settlements (Habitat), *Small Scale Production of Portland Cement*, 1994.

APPENDIX A

Particle Size Distribution of Raw Mix

Raw mix was prepared by mixing soda solid waste, clay and iron ore by certain amounts stated. The particle size granulometry is presented in Figure 11. According to the granulometry, mean diameter of the raw mix was 43.2 micrometer. This attributes to an adequate fineness to obtain a uniform burning.

Result Statistics

Distribution Type: Volume
Concentration = 0.0007 %Vol
Mean Diameters:
D [4, 3] = 43.19 um
D (v, 0.1) = 1.12 um
D [3, 2] = 3.65 um
D (v, 0.5) = 9.64 um
Span = 1.428E+01
D (v, 0.9) = 138.76 um
Uniformity = 4.100E+00

Size (um)	Volume Over %	Size (um)	Volume Over %	Size (um)	Volume Over %	Size (um)	Volume Over %
1.00	91.66	20.00	38.73	75.00	21.41	500.0	0.00
2.00	82.08	25.00	36.23	90.00	17.93	600.0	0.00
3.00	75.86	30.00	34.26	125.0	11.80	700.0	0.00
4.00	70.16	35.00	32.55	150.0	8.71	800.0	0.00
5.00	65.06	40.00	30.98	200.0	4.44		
10.00	49.27	45.00	29.49	300.0	0.55		
15.00	42.44	60.00	25.30	400.0	0.00		

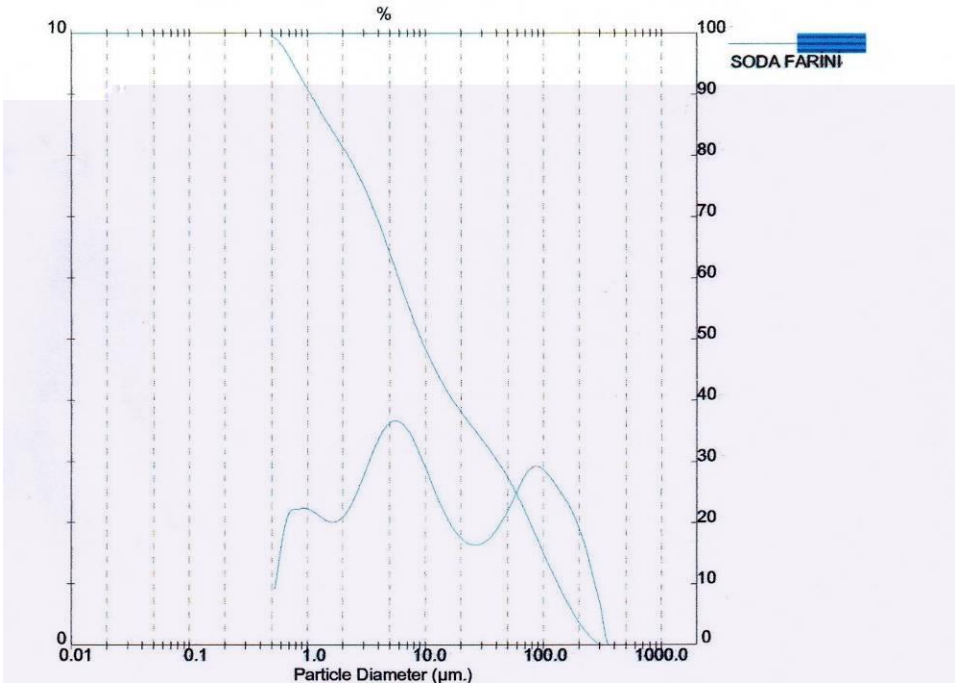

Figure 11 The particle size granulometry of the raw mix

APPENDIX B

XRD Patterns of Samples

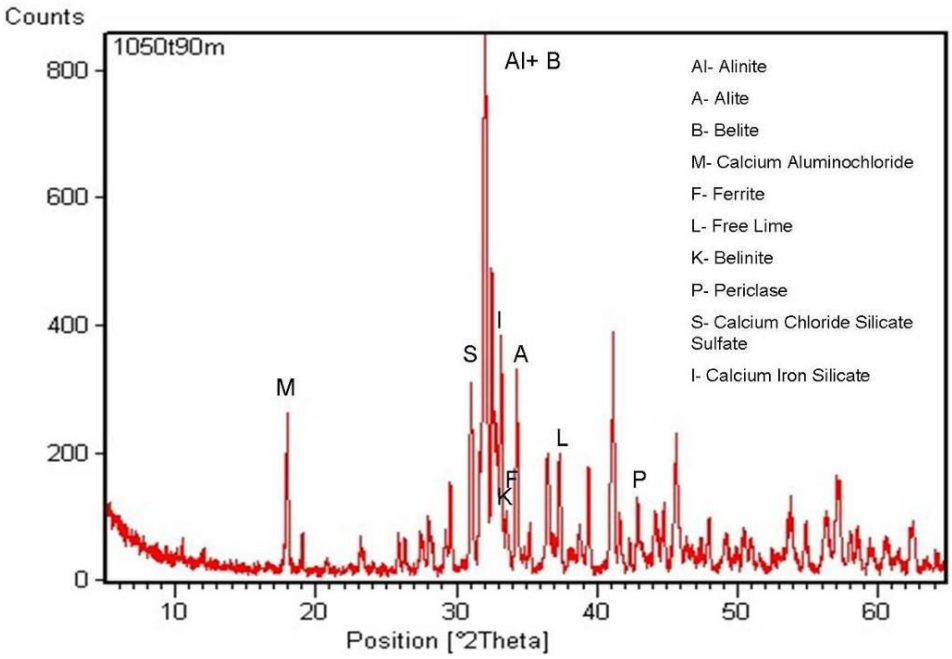

Figure 12 XRD pattern of A1050-90

A1050-90 **Temperature:** 1050ºC **Duration:** 90 min

Alinite [$Ca_{10}Mg_{0.8}[(SiO_4)_{3.4}(AlO_4)_{0.6}O_2Cl]$]

Belite [C_2S]

Calcium Aluminochloride [$C_{11}A_7CaCl_2$]

Ferrite [C_4AF]

Free Lime [CaO]

Belinite [$Ca_8Mg[(SiO_4)_4Cl_2]$]

Periclase [MgO]

Calcium Chloride Silicate Sulfate [$Ca_{10}(SiO_4)_3(SO_4)_3Cl_2$]

Calcium Iron Silicate [$Ca_3Fe_2(SiO_4)_3$], Alite [C_3S]

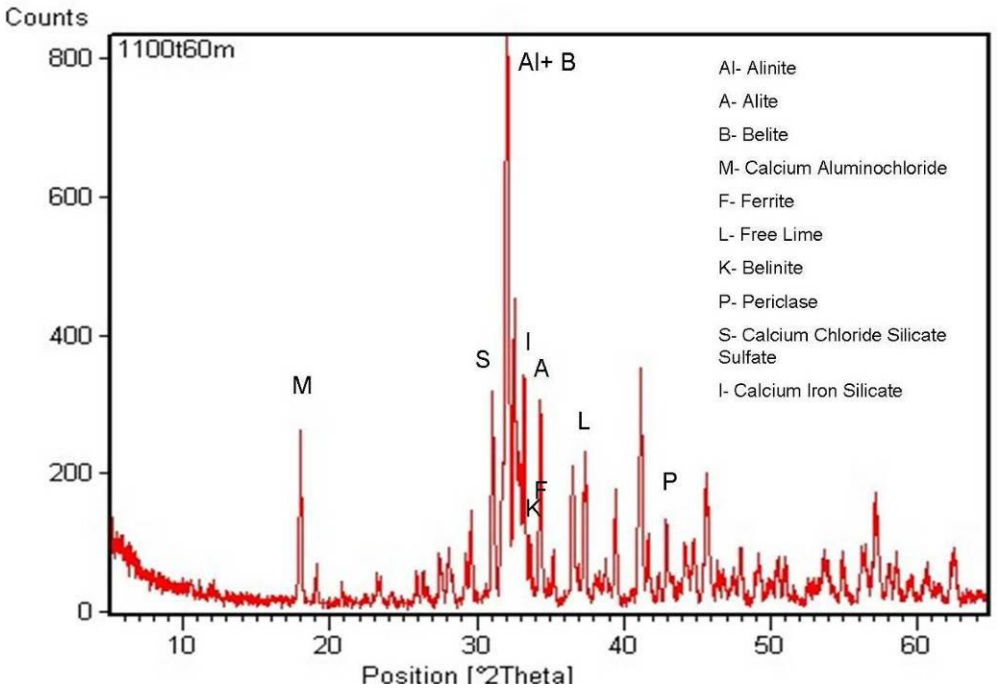

Figure 13 XRD pattern of A1100-60

A1100-60 **Temperature:** 1100ºC **Duration:** 60 min

Alinite [$Ca_{10}Mg_{0.8}[(SiO_4)_{3.4}(AlO_4)_{0.6}O_2Cl]$]

Belite [C_2S]

Calcium Aluminochloride [$C_{11}A_7CaCl_2$]

Ferrite [C_4AF]

Free Lime [CaO]

Belinite [$Ca_8Mg[(SiO_4)_4Cl_2]$]

Periclase [MgO]

Calcium Chloride Silicate Sulfate [$Ca_{10}(SiO_4)_3(SO_4)_3Cl_2$]

Calcium Iron Silicate [$Ca_3Fe_2(SiO_4)_3$]

Alite [C_3S]

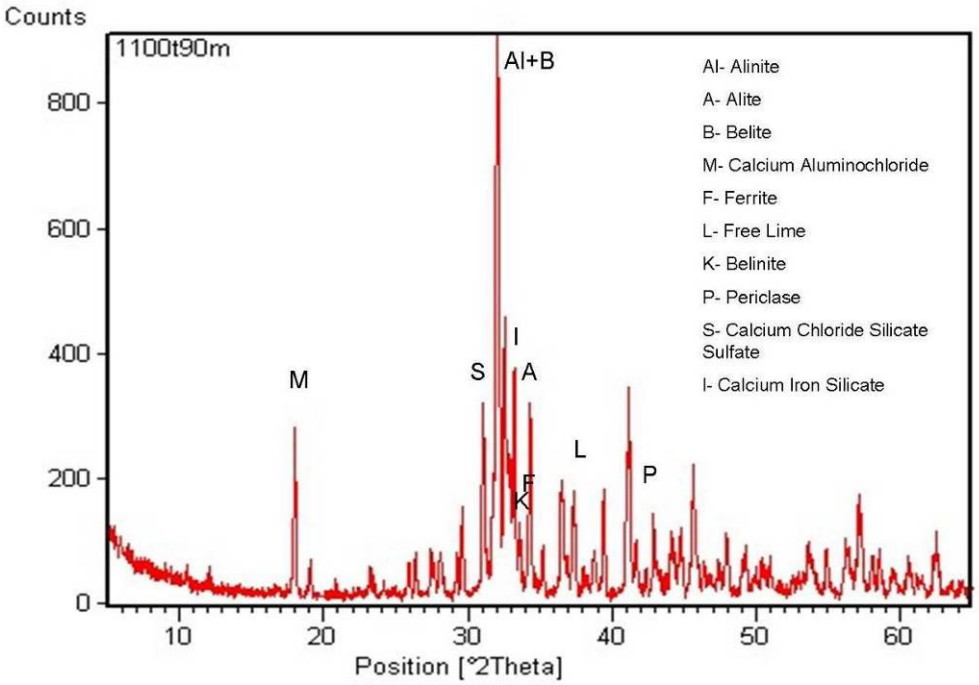

Figure 14 XRD pattern of A1100-90

A1100-90 **Temperature:** 1100ºC **Duration:** 90 min

Alinite [$Ca_{10}Mg_{0.8}[(SiO_4)_{3.4}(AlO_4)_{0.6}O_2Cl]$]

Belite [C_2S]

Calcium Aluminochloride [$C_{11}A_7CaCl_2$]

Ferrite [C_4AF]

Free Lime [CaO]

Belinite [$Ca_8Mg[(SiO_4)_4Cl_2]$]

Periclase [MgO]

Calcium Chloride Silicate Sulfate [$Ca_{10}(SiO_4)_3(SO_4)_3Cl_2$]

Calcium Iron Silicate [$Ca_3Fe_2(SiO_4)_3$]

Alite [C_3S]

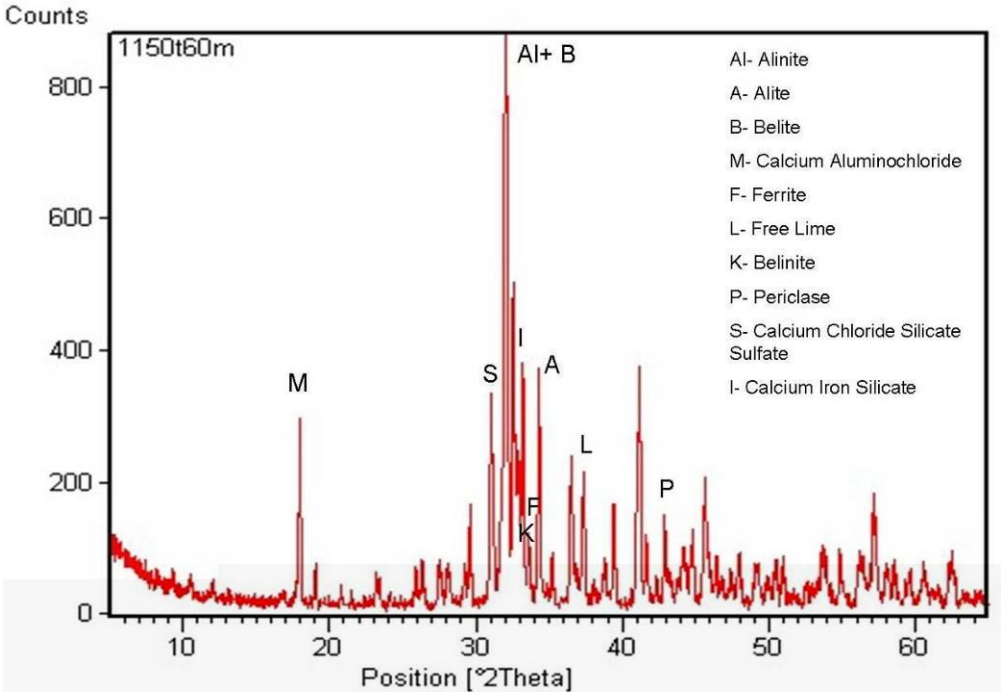

Figure 15 XRD pattern of A1150-60

A 1150-60 **Temperature:** 1150ºC **Duration:** 60 min

Alinite [$Ca_{10}Mg_{0.8}[(SiO_4)_{3.4}(AlO_4)_{0.6}O_2Cl]$]

Belite [C_2S]

Calcium Aluminochloride [$C_{11}A_7CaCl_2$]

Ferrite [C_4AF]

Free Lime [CaO]

Belinite [$Ca_8Mg[(SiO_4)_4Cl_2]$]

Periclase [MgO]

Calcium Chloride Silicate Sulfate [$Ca_{10}(SiO_4)_3(SO_4)_3Cl_2$]

Calcium Iron Silicate [$Ca_3Fe_2(SiO_4)_3$]

Alite [C_3S]

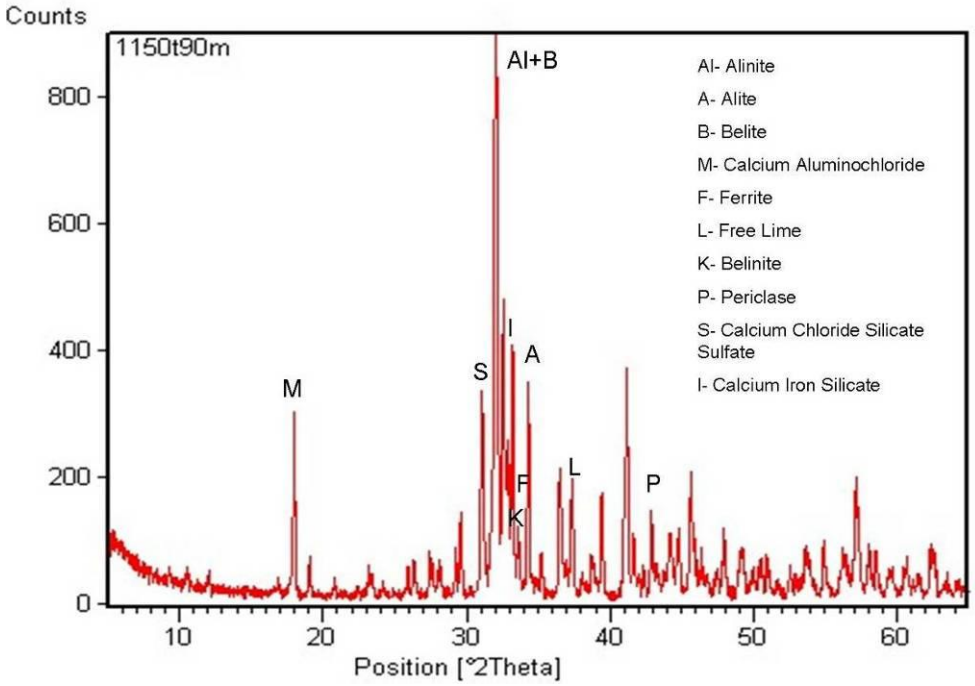

Figure 16 XRD pattern of A1150-90

A 1150-90 **Temperature:** 1150ºC **Duration:** 90 min

Alinite [$Ca_{10}Mg_{0.8}[(SiO_4)_{3.4}(AlO_4)_{0.6}O_2Cl]$]

Belite [C_2S]

Calcium Aluminochloride [$C_{11}A_7CaCl_2$]

Ferrite [C_4AF]

Free Lime [CaO]

Belinite [$Ca_8Mg[(SiO_4)_4Cl_2]$]

Periclase [MgO]

Calcium Chloride Silicate Sulfate [$Ca_{10}(SiO_4)_3(SO_4)_3Cl_2$]

Calcium Iron Silicate [$Ca_3Fe_2(SiO_4)_3$], Alite [C_3S]

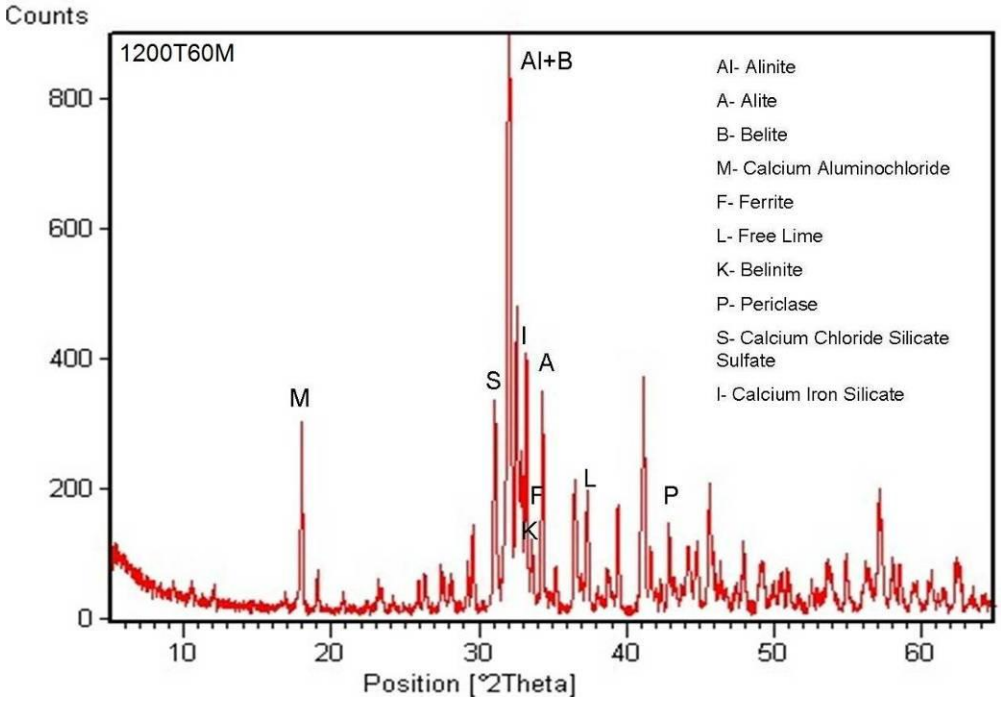

Figure 17 XRD pattern of A1200-60

A1200-60 **Temperature:** 1200ºC **Duration:** 60 min

Alinite [$Ca_{10}Mg_{0.8}[(SiO_4)_{3.4}(AlO_4)_{0.6}O_2Cl]$]

Belite [C_2S]

Calcium Aluminochloride [$C_{11}A_7CaCl_2$]

Ferrite [C_4AF]

Free Lime [CaO]

Belinite [$Ca_8Mg[(SiO_4)_4Cl_2]$]

Periclase [MgO]

Calcium Chloride Silicate Sulfate [$Ca_{10}(SiO_4)_3(SO_4)_3Cl_2$]

Calcium Iron Silicate [$Ca_3Fe_2(SiO_4)_3$]

Alite [C_3S]

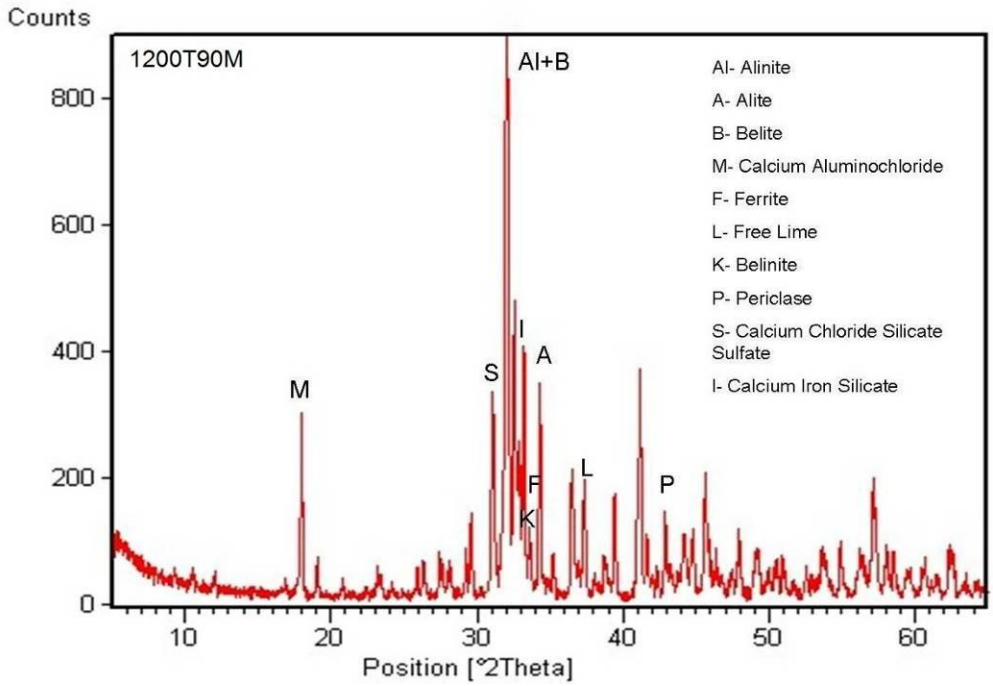

Figure 18 XRD Pattern of A1200-90

A1200-90 **Temperature:** 1200ºC **Duration:** 90 min

Alinite [$Ca_{10}Mg_{0.8}[(SiO_4)_{3.4}(AlO_4)_{0.6}O_2Cl]$]

Belite [C_2S]

Calcium Aluminochloride [$C_{11}A_7CaCl_2$]

Ferrite [C_4AF]

Free Lime [CaO]

Belinite [$Ca_8Mg[(SiO_4)_4Cl_2]$]

Periclase [MgO]

Calcium Chloride Silicate Sulfate [$Ca_{10}(SiO_4)_3(SO_4)_3Cl_2$]

Calcium Iron Silicate [$Ca_3Fe_2(SiO_4)_3$]

Alite [C_3S]

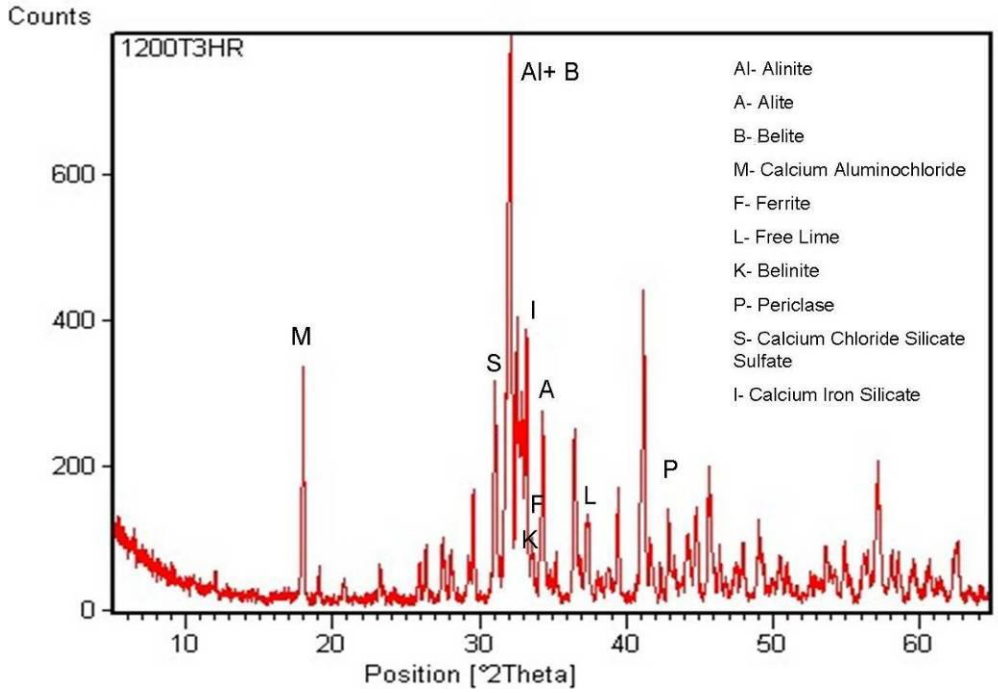

Figure 19 XRD pattern of A1200-180

A1200-180 **Temperature:** 1200ºC **Duration:** 3 h

Alinite [$Ca_{10}Mg_{0.8}[(SiO_4)_{3.4}(AlO_4)_{0.6}O_2Cl]$]

Belite [C_2S]

Calcium Aluminochloride [$C_{11}A_7CaCl_2$]

Ferrite [C_4AF]

Free Lime [CaO]

Belinite [$Ca_8Mg[(SiO_4)_4Cl_2]$]

Periclase [MgO]

Calcium Chloride Silicate Sulfate [$Ca_{10}(SiO_4)_3(SO_4)_3Cl_2$]

Calcium Iron Silicate [$Ca_3Fe_2(SiO_4)_3$]

Alite [C_3S]

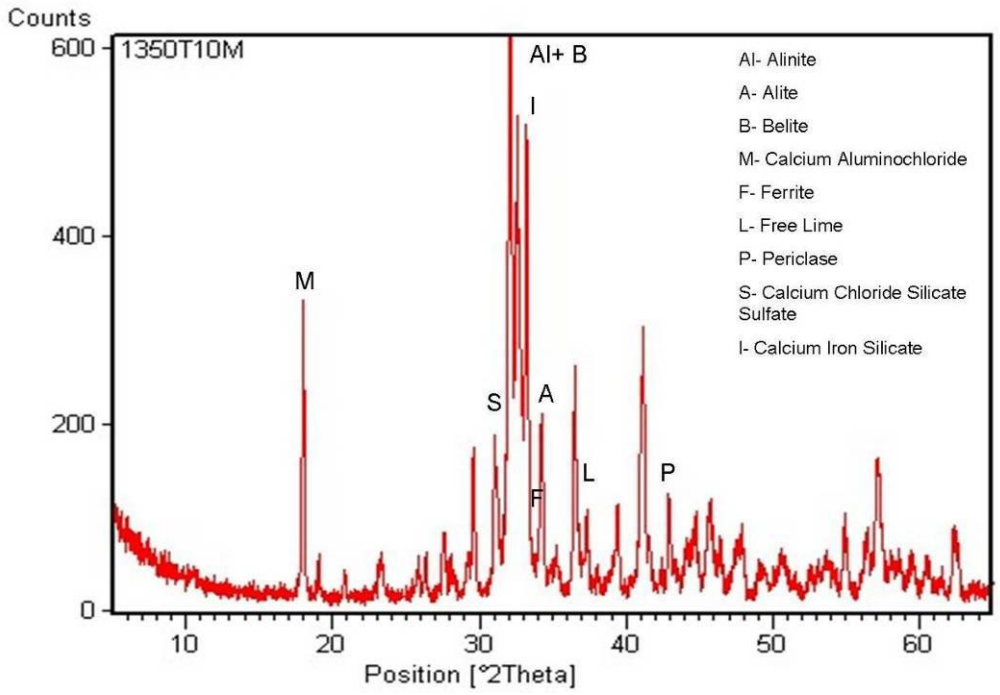

Figure 20 XRD pattern of A1350-10

A1350-10 **Temperature:** 1200ºC **Duration:** 3 h +
Temperature: 1350ºC **Duration:** 10 min

Alinite [$Ca_{10}Mg_{0.8}[(SiO_4)_{3.4}(AlO_4)_{0.6}O_2Cl]$]

Belite [C_2S]

Calcium Aluminochloride [$C_{11}A_7CaCl_2$]

Ferrite [C_4AF]

Free Lime [CaO]

Periclase [MgO]

Calcium Chloride Silicate Sulfate [$Ca_{10}(SiO_4)_3(SO_4)_3Cl_2$]

Calcium Iron Silicate [$Ca_3Fe_2(SiO_4)_3$]

Alite [C_3S]

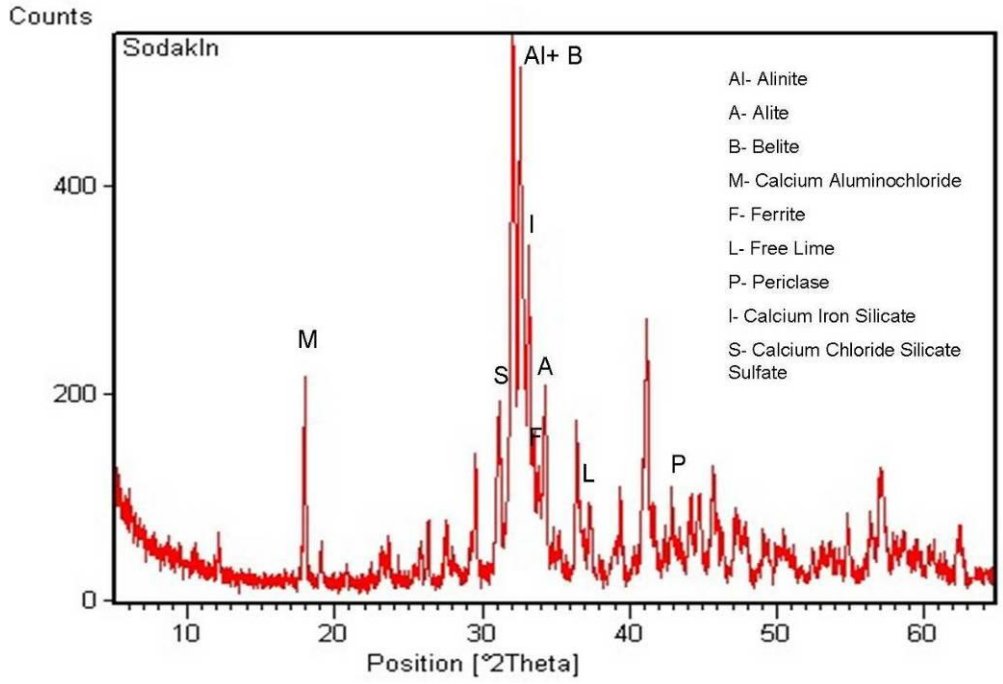

Figure 21 XRD pattern of A1450-10

A1450-10 **Temperature:** 1450ºC **Duration:** 10 min

Alinite [$Ca_{10}Mg_{0.8}[(SiO_4)_{3.4}(AlO_4)_{0.6}O_2Cl]$]

Belite [C_2S]

Calcium Aluminochloride [$C_{11}A_7CaCl_2$]

Ferrite [C_4AF]

Free Lime [CaO]

Periclase [MgO]

Calcium Chloride Silicate Sulfate [$Ca_{10}(SiO_4)_3(SO_4)_3Cl_2$]

Calcium Iron Silicate [$Ca_3Fe_2(SiO_4)_3$]

Alite [C_3S]